University of Alberta

LIPID DYSFUNCTION IN HUNTINGTON DISEASE
- "Molecular Mechanisms and Therapy"

by

Alba Di Pardo

A thesis submitted to the Faculty of Graduate Studies and Research
in partial fulfillment of the requirements for the degree of

Master of Science

Department of Pharmacology

©Alba Di Pardo

Spring 2013
Edmonton, Alberta

Permission is hereby granted to the University of Alberta Libraries to reproduce single copies of this thesis and to lend or sell such copies for private, scholarly or scientific research purposes only. Where the thesis is converted to, or otherwise made available in digital form, the University of Alberta will advise potential users of the thesis of these terms.

The author reserves all other publication and other rights in association with the copyright in the thesis and, except as herein before provided, neither the thesis nor any substantial portion thereof may be printed or otherwise reproduced in any material form whatsoever without the author's prior written permission.

ABSTRACT

Huntington disease (HD) is a neurodegenerative disorder characterized by motor and cognitive symptoms. In HD patients, the protein huntingtin contains an abnormal expansion of a polyglutamine tract, which leads to the selective dysfunction and death of striatal and cortical neurons. Among other cellular dysfunctions, cholesterol and ganglioside GM1 synthesis are affected in HD neurons.

In this thesis I demonstrated that impaired cholesterol metabolism in HD cells results from aberrant interaction of mutant huntingtin with the transcription factor Sterol Regulatory Element-Binding Protein 2 (SREBP2). I also showed that administration of GM1 restores normal motor behavior in HD mice.

My studies have led to a better understanding of the causes of cholesterol metabolism dysregulation in HD, and have identified GM1 as a potential therapy for the disease.

ACKNOWLEDGEMENT

I would like to express my gratitude to all the people who supported me during the last two years as a master student and without whom all this work would not have been possible.

Special thanks to my supervisor Prof. Simonetta Sipione for the interesting project she proposed, her energy, her enthusiasm and continuous support, encouragement and advise necessary for me to proceed through the master program and complete my dissertation. Her guidance helped me in all the time of research and writing of this thesis. It has been a wonderful learning experience working with her. I could not have imagined having a better supervisor and mentor for my studies.

I thank all the members of Sipione's group for the stimulating discussions, for the sleepless nights we were working together before deadlines, and for all the fun we have had in the lab. A special thanks goes to Mel for her efficient technical support and her willingness to help.

I would like to thank also the members of my Supervisory Committee: Prof. Elena Posse De Chaves and Prof. Karim Fouad for their encouragement, insightful comments and helpful suggestions. Their guidance has served me well and I owe them my heartfelt appreciation.

My sincere thanks also goes to all the members of the Lipid Group for allowing me to be part of a great professional community.

I am grateful to Dr. Leslie Thompson (University of California, Irvine) for the kind gift of anti-pSer13 and anti-pSer16 antibodies, Drs. A. Hudson and W. Colmers (University of Alberta) for their assistance with the surgical procedures, and Dr. C. Dickson (University of Alberta) for his advice on statistical analyses.

Also I wish to thank Amany, my friend and colleague for her support and for her constant encouragement throughout my studies and of course for "the other life" outside of the lab with her family, Walid and the little Halim. I will miss the wonderful dinners we have shared and the great time we spent together.

I am grateful to Vittorio whose love and encouragement provided inspiration and was my driving force to finish this journey.

I wish to express my heartiest appreciation to my siblings and my *parents, who have* always *supported me from afar.*

Finally I would thank the Alberta Innovate Health Solution for the financial support provided with my scholarship.

Table of Contents

1. INTRODUCTION 1
1.1. HUNTINGTON DISEASE (HD) 2
1.2. EPIDEMIOLOGY OF HD AND THE DISCOVERY OF HUNTINGTIN (HTT) 4
1.3. MICROSCOPIC PATHOLOGY 4
1.4. MOLECULAR AND CELLULAR PATHOLOGY 5
1.5. MOUSE MODELS OF HUNTINGTON DISEASE 8
1.6. THE CRITICAL ROLE OF LIPIDS IN THE BRAIN 9
1.7. AIMS OF THE THESIS 18
1.8. FIGURES 19
1.9. REFERENCES 25
2. CHAPTER 1 35
DYSREGULATION OF THE CHOLESTEROL BIOSYNTHETIC PATHWAY IN HD 36
2.1. INTRODUCTION 36
2.2. MATERIAL AND METHODS 38
2.3. RESULTS 45

2.4. DISCUSSION 50
2.5. FIGURES 54
2.6. REFERENCES 65

3. CHAPTER 2 68
THERAPEUTIC POTENTIAL OF GANGLIOSIDE GM1 FOR THE TREATMENT OF HD ..69
3.1. INTRODUCTION 69
3.2. MATERIAL AND METHODS 72

3.3. RESULTS 78

3.4. DISCUSSION 82
3.5. FIGURES 85
3.6. REFERENCES 92

4. CONCLUDING REMARKS 97

LIST OF FIGURES

Figure 1.1 Photograph of George Summer Huntington. ……...19

Figure 1.2 Comparison of coronal slices from fixed cerebral hemispheres of an HD patient and matched control subject ……20

Figure 1.3 Overview of the cellular pathogenesis in HD……21

Figure 1.4 Cholesterol biosynthesis pathway……..22

Figure 1.5 SREBP pathway ……....23

Figure 1.6 Simplified scheme of the ganglioside biosynthetic pathway……..24

Figure 2.1 Decreased mature SREBP2 in the nuclear fraction of YAC128 cerebral cortex correlates with decreased SREBP2-dependent gene transcription ……...54

Figure 2.2 Decreased expression of HMG-CoA reductase in the striatum of 9 month-old YAC128 mice……..55

Figure 2.3 mSREBP2-EGFP is mislocalized in the cytoplasm of HD cells….56

Figure 2.4 Immunoblot and densitometric analysis showing the subcellular distribution of transiently transfected mSREBP2-EGFP ……57

Figure 2.5 HMGCoA reductase expression after cell transfection with mSREBP2 is increased to a greater extent in normal than in HD primary fibroblasts. ……58

Figure 2.6 mSREBP1c-EGFP is mislocalized in the cytoplasm of HD cells..59

Figure 2.7 The classic nuclear import is not affected in HD cells……60

Figure 2.8 mSREBP2-EGFP co-localizes with soluble mutant Htt, but is not sequestered into insoluble huntingtin aggregates ……..……61

Figure 2.9 mSREBP2 co-immunoprecipitates with mutant Htt from cytoplasmic fractions of HD cells and brains……62

Figure 2.10 Both wild-type and mutant Htt co-immunoprecipitate with mSREBP2-EGFP from nuclear fractions of HD cells……..63

Figure 2.11 Mutant Htt is in a complex with and stabilizes the interaction between mSREBP2 and importin-! ……...64

Figure 3.1 Chronic GM1 infusion restores normal GM1 levels in the striatum and cortex of YAC128 mice……..85

Figure 3.2 GM1 restores normal motor behavior in YAC128 mice ……..86

Figure 3.3 Sustained beneficial effect of GM1 after treatment discontinuation……...87

Figure 3.4 GM1 restores striatal expression of DARPP-32…… 88

Figure 3.5 GM1 administration elicits huntingtin phosphorylation at serine 13 and serine16……89

Figure 3.6 GM1 administration promotes huntingtin phosphorylation at serine 13 and serine 16 in primary cultures of neurons and human fibroblasts……91

Figure 3.7 GM1 infusion induces huntingtin phosphorylation in vivo……92

LIST OF ABBREVIATIONS

AD	Alzheimer's disease
BBB	Blood-Brain-Barrier
BDNF	Brain Derived Neurotrophic Factor
bHLH-LZ	basic helix–loop–helix leucine zipper (bHLH-LZ
CAG	Cytosine adenine guanin
cAMP	cyclic Adenosine Monophosphate
CNS	Central Nervous System
DARPP-32	Adenosine 3",5"-monophosphate–regulated phosphoprotein
DNA	Deoxyribose nucleic acid
DRP1	Dynamin Related Protein 1
GFP	Green fluorescent protein
HD	Huntington Disease
HMG-CoA	3-Hydroxy-3-methylglutaryl coenzyme A
INSIG 1-2	Insulin-Induced Gene 1-2
IT15	Interesting Transcript 15
mHtt	mutant Huntingtin
MSNs	Medium Size Spiny Neurons
mSREBP	mature SREBP
NPCs	Nuclear Pore Complexes
NMDA	N-methyl-D-aspartate
NMDAR	methyl-D-aspartate (NMDA)-type glutamate receptors
NPC	Niemann–Pick disease type C
NR2B	N-methyl-D-aspartate receptor subunit 2B
NLS	Nuclear Localization Signal
OXPHOS	Oxidative Phosphorylation
PD	Parkinson's disease
PGC1-alpha	Peroxisome proliferator-activated receptor gamma coactivator 1-alpha
polyQ	Polyglutamine
PTP	Permeability Transition Pore
REST	RE1-silencing transcription factor
ROS	Reactive Oxygen Species
S1P	Site 1 protease
S2P	Site 2 Protease
SCAP	SREBP cleavage activation protein
SLOS	Smith-Lemli-Opitz syndrome
Sp1	Specificity Protein 1
SRE	Sterol Response Element

SREBP2	Sterol Regulatory element Binding Protein 2
SREBPs	Sterol Regulatory Element Bindig Proteins
TAFII130	TATA-box-binding protein-associated factor II, 130kDa
TCP-1	Tailless Complex Polypeptide-1
TRiC	ATP-dependent ring-shaped hetero-oligomeric chaperone
YAC	Yeast artificial chromosome

1. INTRODUCTION

1.1. HUNTINGTON DISEASE (HD)

1.1.1. Introduction to the disease

Huntington's Disease (HD) also known as chorea of Huntington, is a fatal brain disease named after George Summer Huntington (Figure 1.1.) who first described the disorder in 1872 (1). The term *chorea* is derived from the Greek word *! " # $ %* (=dance), as the quick movements of the feet or hands are comparable to dancing.

The disease is the most common dominantly inherited neurodegenerative disorder and it is characterized by progressive striatal and cortical neurodegeneration leading to motor, cognitive and behavioral disturbances.

1.1.2. Inheritance

> *'When either or both the parents have shown manifestations of the disease, and more especially when these manifestations have been of a serious nature, one or more of the offspring almost invariably suffer from the disease if they live to adult age. But if by any chance these children go through life without it, the thread is broken and the grandchildren and the great-grandchildren of the original shakers may rest assured that they are free from the disease. This you will perceive differs from the general laws of called hereditary diseases, as for instance in phthisis or syphilis, when one generation may enjoy entire immunity from their dread ravages, and yet in another you find them cropping out in all their hideousness.'*
>
> ***(Huntington 1872)***

A second aspect of hereditary chorea, is dementia and depression. Mood and behavioral disturbance, memory impairment and personality changes are typical clinical features of the disorder, occurring in general before the onset of chorea. However, no universally accepted diagnostic criteria for HD dementia are currently available (2). Psychiatric symptoms like irritability, aggression and psychosis are also common manifestation of the disease that negatively impact upon quality of life and functional capacity (3-4), and are often associated with suicidal ideation (5-6). Suicide attempts are highly frequent in persons carrying the HD mutation, however, these aspects of the disorder are often ignored, as they are less obious than the motor dysfunctions.

> **'***The tendency to insanity, and sometimes that form of insanity which leads to suicide, is marked. I know of several instances of suicide of people suffering from this form of chorea, or who belonged to families in which the disease existed. As the disease progresses the mind becomes more or less impaired, in many amounting to insanity, while in others both mind and body gradually fail until death relieves them of their sufferings. At present I know of two married men, whose wives are living, and who are constantly making love to some young lady, not seeming to be aware that there is any impropriety in it. They are suffering from chorea to such an extent that they can hardly walk and would be thought, by a stranger, to be intoxicated."*
>
> ***(Huntington 1872)***

The disease typically manifests in midlife, with the average onset between 35 and 50 years (7-8). Approximately, 5% to 10% of all HD cases are juvenile forms, with an onset before the age of 20 (9-10).
The progressive motor disorder with uncontrolled and involuntary movements is the most peculiar trait of the disorder.

> *'It begins as an ordinary chorea might begin, by the irregular and spasmodic action of certain muscles, as of the face, arms, etc. These*

movements gradually increase, when muscles hitherto unaffected take on the spasmodic action, until every muscle in the body becomes affected (excepting the involuntary ones), and the poor patient presents a spectacle, which is anything but pleasing to witness. I have never known a recovery or even an amelioration of symptoms in this form of chorea; when once it begins it clings to the bitter end. No treatment seems to be of any avail, and indeed nowadays its end is so well known to the sufferer and his friends, that medical advice is seldom sought. It seems at least to be one of the incurables'.

(Huntington 1872)

1.2. EPIDEMIOLOGY OF HD AND THE DISCOVERY OF HUNTINGTIN (HTT)

Huntington disease is the most prevalent disorder of a family of neurodegenerative diseases that are caused by a polyglutamine expansion in various unrelated proteins (11). HD affects both sexes with the same frequency. The highest prevalence is in Europe and North America, with 4-10 cases per 100.000 (12). An extremely high occurrence was found, for the first time, within the 15.000 members of a large group of inter-related families living in fishing villages along the borders of Lake Maracaibo in Venezuela (13). The first polymorphic DNA marker linked to HD gene locus was discovered in 1983 (14). Ten years later, in 1993, the gene was finally isolated and termed IT15 (interesting transcript 15). The *IT15 gene*, located on the short arm of chromosome 4 (4p16.3) (15) was found to code for huntingtin (Htt), a ubiquitous protein whose function is still unknown (16).

1.3. MICROSCOPIC PATHOLOGY

The neuropathological hallmark of HD is the progressive atrophy of the brain with the striatal medium size spiny neurons (MSNs) and cortical neurons being particularly vulnerable (Figure 1.2) (17). Why these cells

are selectively affected remains unclear, but influence of specific growth factors, excitotoxicity, neurotransmitter gene expression, somatic CAG repeat instability and afferent anatomical connections have been suggested to contribute (18-19). Gross examination of the brain of HD patients reveals atrophy of the caudate nucleus, putamen and dilation of the anterior horns of the lateral ventricles. Beyond the striatum, most brain regions show pathological involvement to some extent. The frontal and prefrontal cortex has long been known to be affected in HD and cortical cell loss has been considered secondary to striatal atrophy (20). Furthermore, other brain regions with potentially important functional links to phenotypic traits of HD have been found to be involved, including the cerebellum (21), hypothalamus (22) and subcortical white matter (23).

1.4. MOLECULAR AND CELLULAR PATHOLOGY

The genetic cause of HD is the expansion of a CAG trinucleotide repeat (>35 repeats) in the gene encoding huntingtin (Htt). The mutation results in an elongated polyglutamine (polyQ) stretch in the N-terminus of the protein. Htt is a 348kDa protein widely expressed within the body. In the brain, it is particularly abundant in the cerebellar cortex, neocortex, striatum and hippocampus (24). Htt is expressed in all brain cells (25) and is required for normal embryogenesis, as knockout mice die at early developmental stages (26). In spite of many years of intense study, the normal function of Htt is still unclear: however it is thought to have diverse functions in vesicle transport, cytoskeletal anchoring, postsynaptic signalling, cytoprotection and transcriptional regulation (27). The expanded polyQ domain in the N-terminal portion of the protein confers toxic properties to mHtt (mHtt) induces protein conformation changes, protein misfolding and aggregation, and results in the disruption of multiple intracellular pathways including cell signaling, mitochondrial

metabolism, neuronal survival and regulation of gene transcription that contribute to neuronal dysfunction and death (28-29) (Figure 1.3).

1.4.1. Altered protein degradation and huntingtin aggregation

In HD and other expanded polyglutamine disorders, neurodegeneration seems to be linked primarily to the neurotoxic “gain of function” of the expanded polyQ stretch. Because of the expanded tract, the mutant protein cannot be properly folded and this results in the formation of aggregates (30). Accumulation and aggregation of disease-causing proteins is a hallmark of several neurodegenerative disorders, including Parkinson’ disease, Alzheimer’ disease, and amyotrophic lateral sclerosis.
Cleavage of mHtt into N-terminal fragments bearing the polyglutamine (polyQ) expansions is believed to contribute to disease pathogenesis. This hypothesis is supported by the observation of N-terminal fragments of mHtt both in HD models and brains from HD patients (31-35). Short fragments may induce toxicity in the cytoplasm by promoting aberrant interactions with proteins and by inducing formation of aggregates. Huntingtin fragments can also translocate from the cytoplasm into the nucleus, where they aberrantly interact with several transcription factors and form protein inclusions (36). The role of aggregates in the progression of HD has been extensively studied, and has yielded a plethora of ambivalent results. While many studies suggest that mHtt aggregates mediate neurotoxicity and may exacerbate neurodegeneration in HD, many others highlight a protective role of aggregates formation, and suggest it is a compensatory detoxification process by which cells promote sequestration of mHtt toxic oligomers (37).

1.4.2. Dysregulation of gene transcription

A number of pathways that have been implicated in the pathogenesis of

HD involve transcriptional dysregulation caused by mHtt. Transcriptional dysregulation has been shown to occur early in HD, before the onset of symptoms (16). The elongated polyglutamine stretch might confer a 'gain of function' property that results in direct and abnormal binding of the mutant protein to DNA disrupting the normal pattern of transcription (38). In addition, mHtt has been reported to aberrantly bind to specific transcription factor proteins thus altering their activity, like in the case of DNA binding specificity protein 1 (Sp1) or TATA-box-binding protein-associated factor II, 130kDa (TAFII130) (39-40). The mutant protein is believed to disrupt transcriptional machinery also through interaction with molecular mediators such as cyclic adenosine monophosphate (cAMP) response element binding protein (CBP) or p300/CBP associated factor, which affect histone acetylation, chromatin structure and gene transcription (41). Microarray studies conducted in HD models and in postmortem brain samples from HD patients have revealed a decrease in the expression of several genes necessary for neuronal function and survival, including the Brain Derived Neurotrophic Factor (BDNF), the co-activator Peroxisome proliferator-activated receptor gamma coactivator 1-alpha (PGC1-alpha), and cholesterogenic genes (41-46).

1.4.3. Dysfunction of mitochondrial activity

The mechanisms underlying neuronal vulnerability in HD are still unknown, however, evidence suggests that mitochondrial defects may play a central role. Mitochondrial dysfunction in HD has been demonstrated in numerous studies (47) and includes aberrant mitochondrial Ca^{2+} storage and handling, decreased expression of oxidative phosphorylation (OXPHOS) enzymes, production of reactive oxygen species (ROS) and loss of membrane potential (48). Although it is still unclear how mHtt interferes with normal mitochondrial activity, many studies indicate that mHtt can act at the transcriptional level, by inhibiting PGC1-alpha, the master regulator of energy homeostasis, and by affecting the function of dynamin related

protein 1 (DRP1) and causing fragmentation and remodeling of the mitochondrial cristae. Other transcriptional abnormalities affecting mitochondria composition, reduced mitochondria trafficking to synapses, and direct interference with mitochondria may also contribute to striatal vulnerability in HD.

1.4.4. Cytotoxicity

Excitotoxicity was the first mechanism of neurodegeneration proposed for HD (49). The excitotoxic hypothesis in HD is supported by several studies showing excessive activation of N-methyl-D-aspartate (NMDA)-type glutamate receptors (NMDAR) in HD models, potentially due to increased glutamate release from cortical afferents and reduced uptake of glutamate by glia (50-53). Several studies have reported selective potentiation of striatal NR2B-containing NMDAR activity and concomitant early increase in extrasynaptic NMDAR activity, with subsequent exacerbation of striatal neurodegeneration in HD mouse models (54). Notably, overactivation of NMDAR is associated with an increase of intracellular free calcium levels in MSNs (55). While activation of extrasynaptic NMDARs is detrimental, the activity of synaptic NMDARs is protective in HD mice, and it correlates with the formation of non-toxic mHtt inclusion bodies by a process involving the transcriptional up-regulation of chaperonin tailless complex polypeptide-1 (TCP-1) and promotes cell survival (56).

1.5. **MOUSE MODELS OF HUNTINGTON DISEASE**

Researchers are using animal models of HD to study the disease pathogenesis, to elucidate areas of the brain involved in structural and functional decline, and to evaluate potential therapeutic interventions. The most reliable models of HD principally recapitulate the neuropathology in the striatum, as well as the genetic defect and symptomology of the human disease.

Transgenic mice that express the mHtt gene, or portions of it, have

been the most commonly used animal models to investigate the molecular mechanisms underlying the disease and potential therapies. Several genetic mouse models of HD have been developed, using a variety of gene promoters and expressing Htt fragments and polyQ expansions of various lengths.

Transgenic mice expressing the first exon of *Htt* with 155 CAG repeats (strain line R6/2), are the most commonly used transgenic mouse model of HD. The large number of repeats in the R6/2 model corresponds to a juvenile onset HD in patients. This model has a very severe phenotype and fast disease progression. R6/2 mice may develop symptoms as early as 4 weeks of age, although the average age at onset of symptoms is 9 to 11 weeks. These mice rarely survive past 14 weeks of age (57).

The yeast artificial chromosome (YAC) mouse model expresses full-length human Htt with 128 CAG repeats (YAC128) from the human *Htt* promoter. This model accurately recapitulates age-dependent brain atrophy, including cortical and striatal atrophy, and striatal neuronal loss characteristic of HD (58). The onset of impairment in motor co-ordination, in pre-pulse inhibition and cognition, along with a biphasic activity profile composed of initial hyperactivity and late hypoactivity in the YAC128 mice recapitulates the clinical manifestation of the human disease. YAC128 mice have been extensively used for the study of pathogenic mechanisms in HD, as well as to test therapeutics. The longer life-span of YAC128 mice, compared to other HD models, allows for their use to study the effects of long-term therapeutic interventions.

1.6. THE CRITICAL ROLE OF LIPIDS IN THE BRAIN

Lipids are the most abundant component of the Central Nervous System (CNS). They comprise a large number of chemically distinct molecules arising from combination of fatty acids with various backbone structures. Overall, mammalian cells may contain approximately 1000-2000 lipid species (59).

They are classified into eight categories (fatty acids, glycerolipids, glycerophospholipids, sphingolipids, sterol lipids, prenol lipids, saccharolipids and polyketides) (60) and all increase during development. Among all the lipids, cholesterol and gangliosides are highly enriched in the brain. Both cholesterol and gangliosides are essential component of membrane micro-domains that serve as hubs for cell signaling and are crucial for many brain functions. They are involved in major biological processes such as intracellular transport, membrane trafficking, signaling transduction as well as myelin formation and maintenance, and synaptogenesis.

The importance of cholesterol and gangliosides in the CNS is underlined by the fact that perturbations of the metabolism of these lipids negatively affect neuronal function and causes a number of neurodegenerative disorders (61, 62). The maintenance of balanced lipid homeostasis is, therefore, an important aspect of CNS function (63, 61) and it is critical during neurodevelopment, repair after traumatic brain injury and for the maintenance of efficient neurotransmission.

1.6.1. Cholesterol

5-Cholesten-3! -ol or cholesterol is the main sterol synthesized by animal cells. Although it represents only two percent of total body mass, the brain contains the highest levels of cholesterol in mammalian bodies. Approximately 25% of the total amount of the cholesterol present in humans is localized in the brain. Cholesterol has a number of crucial functions in the brain. Brain cholesterol is synthesized locally and is metabolically separated from other pools by the blood-brain-barrier (BBB) (63). Thus, dietary and peripherally-synthesized cholesterol cannot be utilized by brain cells. Cholesterol homeostasis is tightly regulated in the brain as well as in the rest of the body, and depends on three main aspects: synthesis, transport and catabolism.

Cholesterol biosynthesis is a multi-step process involving nearly 30

enzymes and is directly regulated by intracellular cholesterol levels (Figure 1.4). The rate-limiting step of this pathway is the production of mevalonate by the enzyme 3-hydroxy-3-methylglutaryl coenzyme A (HMG-CoA) reductase (HMGCR). HMGCR is a glycoprotein, anchored to the ER membrane and is one of the most highly regulated enzymes. HMGCR is subject to numerous modes of regulation, including feedback control of HMGCR stability (64-66). HMGCR reductase expression levels are regulated in response to sterols both transcriptionally, through a complex regulatory loop involving the ER Insig proteins, and posttranslationally by Insig-dependent protein degradation by the ubiquitin-proteasome system. Increased production of products of the mevalonate pathway causes an increase in the degradation rate of HMGCR by the proteosome and lowered steady-state level of the protein (64). Conversely, decreased production of pathway products causes a decrease in the degradation rate of HMGCR and increased steady-state levels of the protein. The primary sterol regulating HMGCR degradation is cholesterol itself. As the levels of free cholesterol increase in cells, the rate of HMGCR degradation increases.

At the transcriptional level, the mevalonate pathway is regulated by a subfamily of basic helix–loop–helix leucine zipper (bHLH-LZ) transcription factors the sterol regulatory element binding proteins (SREBPs) (67). SREBPs directly activate the expression of a number of genes dedicated to the synthesis and uptake of cholesterol, fatty acids, triglicerides and phospholipids (68, 69).

In the adult brain, astrocytes are the major site of cholesterol synthesis (70). In early developmental stages, neurons can synthesize cholesterol them selves. In contrast, mature neurons rely on astrocytes for the energy consuming process of cholesterol biosynthesis (70, 71). Astrocytes synthesize and secrete cholesterol in order to supply neurons with the cholesterol that is needed for the formation of new synapses, axonal outgrow and vesicle exocytosis, which are all essential for learning and

memory processes (72, 73). Neither peripheral cholesterol nor brain cholesterol can cross the BBB. Therefore, elimination of excess cholesterol from the brain occurs after cholesterol is metabolized into the oxysterol 24(S)-OH cholesterol, a more soluble sterol that is able to traverse the BBB (74). The role of cholesterol in the brain is complex and the maintenance of balance cholesterol homeostasis is an important aspect of CNS function (75). Smith-Lemli-Opitz syndrome (SLOS) is a well characterized and the most common disease caused by defects in cholesterol metabolism (76). The clinical manifestations of SLOS may result from cholesterol deficiency or from the toxicity of accumulation of precursor sterols and their toxic metabolites (76). Deregulated cholesterol homeostasis appears to be involved in the pathogenesis of a number of neurodegenerative disorders including Alzheimer's disease (AD), Parkinson's disease (PD) and Niemann–Pick disease type C (NPC) diseases (77, 78), and interestingly also in HD (79, 80).

1.6.2. Sterol regulatory element binding proteins (SREBPs)

The synthesis and uptake of cholesterol in animal cells require membrane-bound transcription factors designated as sterol-regulatory element-binding proteins (SREBPs) (81, 82). SREBPs activate the expression of numerous genes that regulate not only the synthesis and uptake of cholesterol, but also the synthesis of fatty acids, triglycerides, and phospholipids (83, 84). SREBPs belong to the basic helix-loop-helix–leucine zipper (bHLH-Zip) family of transcription factors but they differ from other bHLH-Zip proteins in that they are synthesized as inactive precursors bound to the endoplasmic reticulum (ER) (83, 84). The mammalian genome encodes three SREBP isoforms: SREBP-1a, SREBP-1c, and SREBP-2. SREBP-2 is encoded by a gene on human chromosome 22q13. Both SREBP-1a and -1c are derived from a single

gene on human chromosome 17p11.2 through the use of alternative transcription start sites that produce alternate forms of exon 1, 1a and 1c (83). SREBP-1a is a potent activator of all SREBP-responsive genes, including those that mediate the synthesis of cholesterol, fatty acids, and triglycerides. SREBP-1c preferentially enhances transcription of genes required for fatty acid synthesis but not cholesterol synthesis. Like SREBP-1a, SREBP-2 has a long transcriptional activation domain and it preferentially activates cholesterol synthesis (83). In order to enter the nucleus and act as a transcription factor, the NH2-terminal domain of each SREBP must be cleaved and released by specific proteases (Figure 1.5). Three proteins are required for SREBP processing: one is an escort protein designated SREBP cleavage–activating protein (SCAP). The other two are proteases, designated Site-1 protease (S1P) and Site-2 protease (S2P). Newly synthesized SREBP is inserted into the membranes of the ER, where its COOH-terminal regulatory domain binds to the COOH-terminal domain of SCAP. SCAP is both an escort for SREBPs and a sensor of sterols. When cells become depleted in cholesterol, SCAP escorts SREBP from the ER to the Golgi apparatus, where the two proteases reside. In the Golgi apparatus, S1P, a membrane-bound serine protease, cleaves SREBP (Figure 1.5). The NH2-terminal bHLH-Zip domain is then released upon intra-membrane proteolysis via a second cleavage mediated by S2P, a membrane-bound zinc metalloproteinase. The NH2-terminal domain, designated nuclear or “mature” SREBP (mSREBP), enters the nucleus and activates transcription, by binding to sterol response elements (SREs) in the promoter regions of target genes. The nuclear content of SREBPs declines rapidly as a result of proteasomal degradation to maintain a tight control of cholesterol and fatty acids synthesis.

1.6.3. Nuclear transport

Transport of macromolecules into and out of the nucleus occurs through large structures called nuclear pore complexes (NPCs) (85). Nuclear pore complexes allow passive diffusion of ions and small proteins (<40 kDa), but restrict passage of large molecules, the transport of which is an active process (86).

The active transport of macromolecular cargo between cytoplasmic and nuclear compartments is facilitated by specific soluble carrier proteins referred to as “karyopherins” (87), with those involved in import and export termed “importins” (88) and “exportins” (89), respectively.

Cytosolic proteins bearing a classical nuclear localization signal (NLS) enter the nucleus bound to a heterodimer of importin-# and importin-! (90). The importin #/! heterodimer targets hundreds of nuclear proteins that contain the classic nuclear localization signals (NLSs) (91) to the nuclear-pore complex (NPC) and mediates the classical nuclear transport by facilitating proteins translocation across the nuclear envelope. In the classical nuclear import importin-# recognizes and binds NLS-containing cargos and forms a complex with importin-! (92). Importin-! then mediates interaction of the trimeric complex with the phenylalanine–glycine (FG) repeat domains of nucleoporins, in the nuclear pore complex, as it translocates into the nucleus. In the nucleus, binding of RanGTP to importin-! causes a conformational change in the latter protein that results in the release of the cargo from the complex (93).

Although most nuclear proteins follow the simple model of classical nuclear transport to enter nucleus, a few proteins are transported through a non-classical nuclear transport characterized by direct interaction of the cargo protein to importin-! . This alternative mode of nuclear entry is quite unique for SREBPs and a few other proteins (94, 95)

1.6.4. Gangliosides

Gangliosides are sialic acid-containing glycosphingolipids ubiquitously expressed in the outer leaflet of the plasma membrane of the cells of all vertebrates and are particularly abundant in the nervous system (96). The synthesis of gangliosides occurs through a complex metabolic pathway that involves many enzymes (Figure 1.6).

Unlike cholesterol biosynthesis, the factors that regulate *de novo* gangliosides biosynthesis for the most part remains enigmatic; this pathway does not appear to require a single class of master transcriptional regulators, or respond solely to cellular sphingolipid concentrations (97).

Gangliosides are primarily localized in the outer leaflets the plasma membranes and are integral components of membrane microdomains or “lipid rafts” along with proteins, sphingomyelin and cholesterol. They participated in a number of essential biological processes including neurite outgrowth (98) cell–cell recognition and interaction adhesion and signal transduction (99), through modulation of membrane receptors and/or downstream signaling pathways (100).

Expression levels and patterns of brain gangliosides are known to change dramatically during development. For instance, the amount of total gangliosides increases almost 8-fold in adult mouse brains as compared with embryonic mouse brains (101). Simultaneously, the expression pattern of gangliosides shifts from simple gangliosides, such as GM3 and GD3, to complex gangliosides, such as GM1, GD1a, GD1b, and GT1b. Similarly, in the human brain, the amount of ganglioside increases approximately 3-fold from the gestational weeks to the infant period. GM1 and GD1a are increased 12- to 15-fold during the same period (102). Gangliosides homeostasis is of vital importance in the CNS. As a matter of fact, defects in gangliosides synthesis cause severe neurological and neurodegenerative conditions (103).

Disruption of ganglioside synthetic genes induces developmental defects and neural degeneration. Deficiency of GM2/GD2 synthase leads to

impaired motor development, seizure and death in infancy (103). Loss-of-function mutation in the gene encoding GM3 synthase leads to a severe infantile neurodegenerative disorder characterized by progressive brain atrophy, epilepsy and chorea (104), symptoms that are also common to the juvenile form of HD (105). Aberrant gangliosides metabolism has also been described in AD and in HD (106, 107).

1.6.5. Dysfunction of cholesterol and ganglioside metabolism in Huntington disease

Among other dysfunctions that play a critical role in the pathogenesis of HD, disturbances in cholesterol and ganglioside homeostasis have been described in HD patients and animal models of the disease, raising the question of how changes in lipid metabolism might contribute to HD pathogenesis.

Down-regulation of expression of key genes involved in cholesterol synthesis, such as HMGCR, Cyp51 and 7-dehydroxycholesterol reductase, was first reported in a study that analyzed global gene expression changes upon expression of mHtt in striatal cell lines (46).

Further studies described similar changes in brain tissues of HD mouse models before the onset of motor and cognitive symptoms (108-110) suggesting that decreased cholesterol biosynthesis might play a role in the pathogenesis of the disease. Changes in the cholesterol content instead, were detected only at more advanced symptomatic stages (108-110)

Expression of mRNA for cholesterol biosynthetic genes was found to be reduced also in fibroblasts and post mortem striatal and cortical tissues from patients with HD (108).

Despite several studies have highlighted defective cholesterol synthesis in HD, very little attention has been paid to the underlying molecular mechanisms.

The available data indicate that the decreased cholesterol biosynthesis in HD is attributable to the interference of mHtt with the function of SREBP2 (108) although how exactly this is achieved is not clear.

Defects in cholesterol metabolism in various models of HD are also accompanied by abnormal ganglioside metabolism, although it is currently unknown whether these two dysfunctions are linked to each other.

Alteration in ganglioside concentration in the caudate and putamen of HD patients were first reported prior to the identification of HD gene (111). Later microarray data from the R6/1 mouse model of HD and from postmortem human caudate samples of HD patients, revealed a decrease in the expression of genes involved in glycosphingolipid synthesis, relative to disease-free controls (112). In line with these findings, our lab reported defects in ganglioside metabolism associated with transcriptional dysregulation of the ganglioside biosynthetic genes in various HD models and in fibroblasts from HD patients. We also showed that decreased levels of gangliosides GM1 contributes to increased susceptibility of HD cells to apoptosis (107) and that administration of exogenous GM1 dramatically increases cell survival in HD (107). These results are in agreement with previous studies reporting that administration of ganglioside GM1 has neuroprotective properties in models of other neuronal injury by growth factor withdrawal (113) or excitotoxicity (114), as well as in primate models of Parkinson's disease (115) and in stroke (116).

Although additional research is needed to clarify how ganglioside and cholesterol alterations contribute to human pathology, all together the information available suggest that aberrant metabolism of cholesterol and gangliosides may significantly contribute to the onset and development of HD. A better understanding of the precise impact of such dysfunctions in HD and of the underlying mechanisms might eventually guide the development of potential new therapeutic approaches for the treatment of this disease.

1.7. AIMS OF THE THESIS

The aims of this thesis were: 1) to elucidate the mechanism by which mHtt interferes with cholesterol synthesis and 2) to determine whether strategies that increase brain ganglioside levels have therapeutic potential in HD.

Chapter II describes experiments that shed light on the causes of defective cholesterol biosynthesis in HD.

In **chapter III** I describe the effects of exogenous ganglioside GM1 administration in a mouse model of HD, and I provide evidence that GM1 is a potential and innovative approach for the treatment of HD.

1.8. **FIGURES**

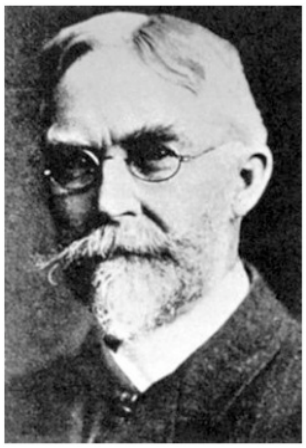

Figure 1.1 Photograph of George Summer Huntington. Born 1850, East Hampton, New York, USA –1916, died in Cairo, New York, USA (Okun, 2003).

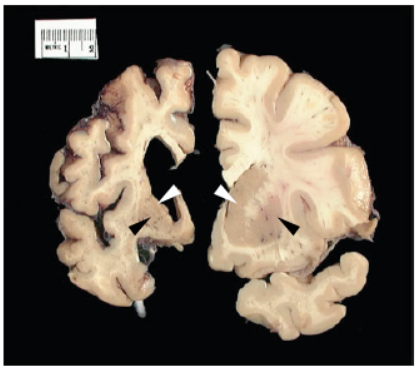

Figure 1.2. Comparison of coronal slices from fixed cerebral hemispheres of an HD patient and matched control subject. HD patient on left, control subject on right. White arrowheads, caudate nuclei; black arrowheads, putamina. Image courtesy of Harvard Brain Tissue Resource Center.

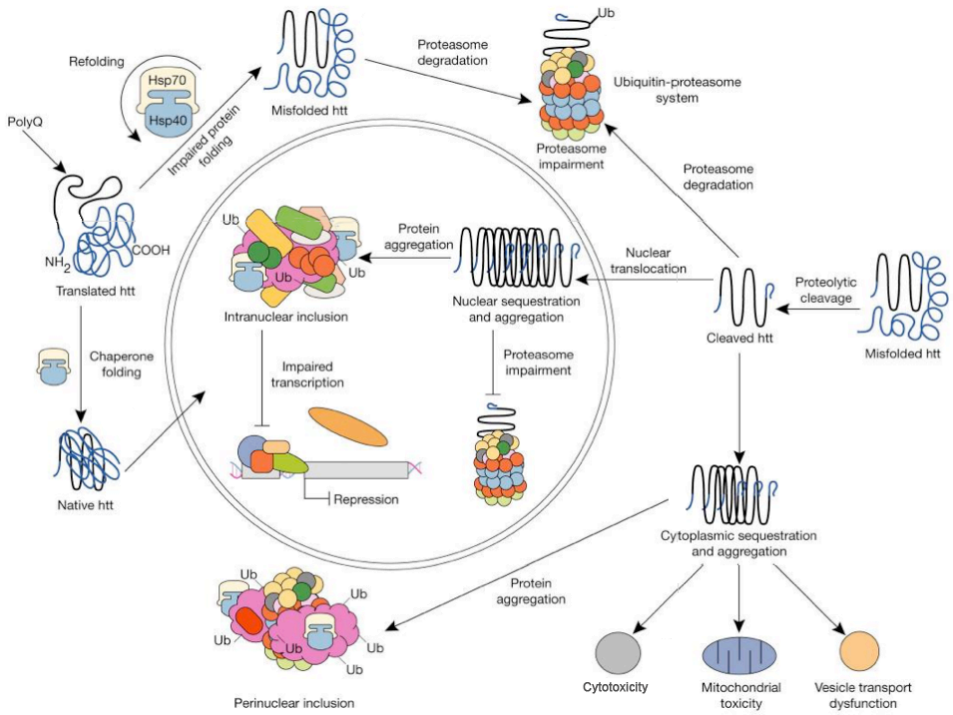

Figure 1.3. Overview of the cellular pathogenesis in HD. Htt, huntingtin; Ub, ubiquitin (Adapted from Landles et al. 2004).

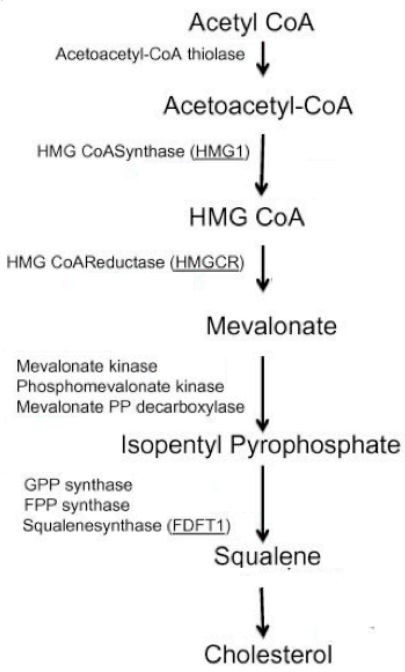

Figure 1.4. Cholesterol biosynthesis pathway. A biochemical pathway showing the major steps by which cholesterol is synthesized.

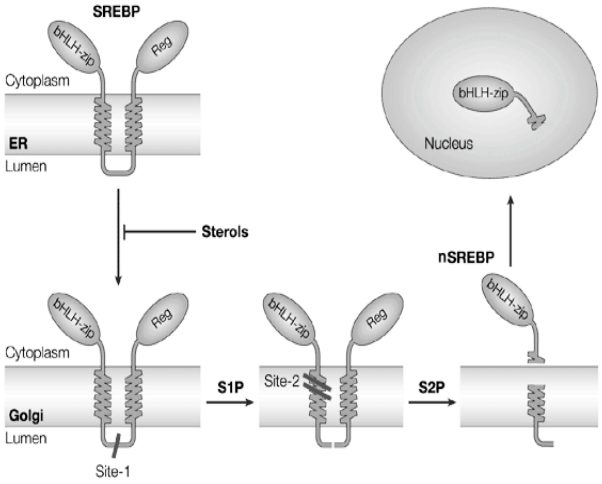

Figure 1.5. SREBP pathway. SREBP precursor is inserted in the membranes of the endoplasmic reticulum (ER). Both the amino-terminal transcription-factor domain (bHLH-zip) and the carboxy-terminal regulatory domain (Reg) are located in the cytoplasmic compartment. When the cellular demand for sterols rises, the SREBP precursor protein travels to the Golgi apparatus, where the site-1 protease (S1P) cleaves at site-1 in the luminal loop, producing the membrane-bound intermediate form. The intermediate form is the substrate for the site-2 protease (S2P), which cleaves the intermediate at site-2. This second cleavage releases the mature transcription-factor domain (mSREBP) from the membrane, freeing it to enter the nucleus and direct transcription of target genes. bHLH-zip, basic helix–loop–helix leucine-zipper. (*Adapted from Rawson RB. 2003*)

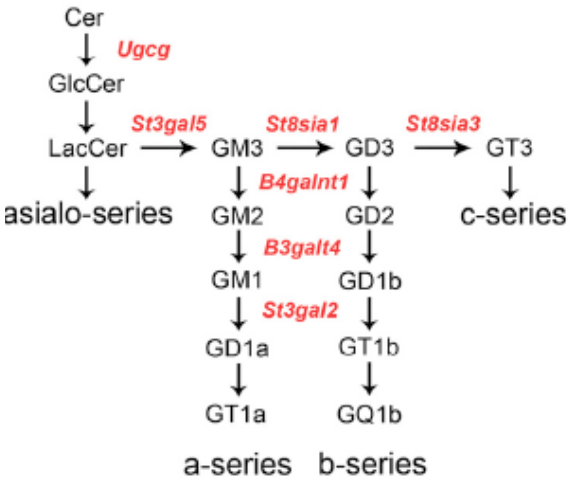

Figure 1.6. Simplified scheme of the ganglioside biosynthetic pathway. Critical enzymes in the pathway are indicated in red**.** Ceramide (Cer); glucosylceramide (GlcCer); lactoceramide (LacCer) Trisialotetrahexosylganglioside (GM3); Disialotetrahexosylganglioside (GM2)*;* Monosialotetrahexosylganglioside (GM1); Ganglioside GD1a; Ganglioside GT1a; Ganglioside Precursor Disialohematoside (GD3); Ganglioside GD2; Ganglioside GD1b; Ganglioside GT1b; Ganglioside GQ1b; Tri-sialosyllactosylceramide (GT3).

1.9. **REFERENCES**

1. Huntington G. (2003) On chorea. George Huntington, M.D. J Neuropsychiatry Clin Neurosci. Winter;15(1):109-12.
2. Paulsen JS (2011). Cognitive impairment in Huntington disease: diagnosis and treatment. Curr Neurol Neurosci Rep. Oct;11(5):474-83.
3. Reedeker N, Bouwens JA, van Duijn E, Giltay EJ, Roos RA, van der Mast RC. (2011) Incidence, course, and predictors of apathy in Huntington's disease: a two-year prospective study. J Neuropsychiatry Clin Neurosci. Fall;23(4):434-41.
4. Orth M; European Huntington's Disease Network, Handley OJ, Schwenke C, Dunnett S, Wild EJ, Tabrizi SJ, Landwehrmeyer GB. (2011) Observing Huntington's disease: the European Huntington's Disease Network's REGISTRY. J Neurol Neurosurg Psychiatry. Dec;82(12):1409-12.
5. Hubers AA, Reedeker N, Giltay EJ, Roos RA, van Duijn E, van der Mast RC. (2012) Suicidality in Huntington's disease. J Affect Disord. Feb;136(3):550-7.
6. Wetzel HH, Gehl CR, Dellefave-Castillo L, Schiffman JF, Shannon KM, Paulsen JS; Huntington Study Group (2011). Suicidal ideation in Huntington disease: the role of comorbidity. Psychiatry Res. Aug 15;188(3):372-6.
7. Quinn N, Schrag A. Huntington's disease and other choreas. (1998) J Neurol. Nov;245(11):709-16.
8. Ross CA, Tabrizi SJ. (2011) Huntington's disease: from molecular pathogenesis to clinical treatment. Lancet Neurol. Jan;10(1):83-98.
9. Farrer LA, Conneally PM. (1985) A genetic model for age at onset in Huntington disease. Am J Hum Genet. Mar;37(2):350-7.
10. Nance MA. (1997) Genetic testing of children at risk for Huntington's disease. US Huntington Disease Genetic Testing Group. Neurology. Oct;49(4):1048-53.
11. Takahashi T, Katada S, Onodera O (2010). Polyglutamine diseases: where does toxicity come from? what is toxicity? where are we going? J Mol Cell Biol. Aug;2(4):180-91.
12. Squitieri F, Andrew SE, Goldberg YP, Kremer B, Spence N, Zeisler J, Nichol K, Theilmann J, Greenberg J, Goto J. (1994). DNA haplotype analysis of Huntington disease reveals clues to the origins and mechanisms of CAG expansion and reasons for geographic variations of prevalence. Hum Mol Genet. Dec;3(12):2103-14.
13. Okun MS, Thommi N. (2004) Americo Negrette (1924 to 2003): diagnosing Huntington disease in Venezuela. Neurology.Jul 27;63(2):340-3.

14. Gusella JF, Wexler NS, Conneally PM, Naylor SL, Anderson MA, Tanzi RE, Watkins PC, Ottina K, Wallace MR, Sakaguchi AY. (1983) A polymorphic DNA marker genetically linked to Huntington's disease. Nature. Nov 17-23;306(5940):234-8.
15. A novel gene containing a trinucleotide repeat that is expanded and unstable on Huntington's disease chromosomes. (1993) The Huntington's Disease Collaborative Research Group. Cell.Mar 26;72(6):971-83.
16. Zuccato C, Valenza M, Cattaneo E (2010). Molecular mechanisms and potential therapeutical targets in Huntington's disease. Physiol Rev. Jul;90(3):905-81.
17. Vonsattel JP, Keller C, Del Pilar Amaya M. (2008) Neuropathology of Huntington's disease. Handb Clin Neurol. 89:599-618.
18. Sieradzan KA, Mann DM. (2001) The selective vulnerability of nerve cells in Huntington's disease. Neuropathol Appl Neurobiol. Feb;27(1):1-21.
19. Gonitel R, Moffitt H, Sathasivam K, Woodman B, Detloff PJ, Faull RL, Bates GP. (2008) DNA instability in postmitotic neurons. Proc Natl Acad Sci U S A. Mar 4;105(9):3467-72.
20. Cudkowicz M, Kowall NW. (1990) Degeneration of pyramidal projection neurons in Huntington's disease cortex. Ann Neurol. Feb;27(2):200-4.
21. Jeste DV, Barban L, Parisi J. (1984) Reduced Purkinje cell density in Huntington's disease. Exp Neurol. Jul;85(1):78-86.
22. Kremer B, Tallaksen-Greene SJ, Albin RL. (1993) AMPA and NMDA binding sites in the hypothalamic lateral tuberal nucleus: implications for Huntington's disease. Neurology. Aug;43(8):1593-5.
23. Halliday GM, McRitchie DA, Macdonald V, Double KL, Trent RJ, McCusker E. (1998) Regional specificity of brain atrophy in Huntington's disease. Exp Neurol. Dec;154(2):663-72.
24. Schmitt I, Bächner D, Megow D, Henklein P, Hameister H, Epplen JT, Riess O. (1995) Expression of the Huntington disease gene in rodents: cloning the rat homologue and evidence for downregulation in non-neuronal tissues during development. Hum Mol Genet. Jul;4(7):1173-82.
25. Sapp E, Schwarz C, Chase K, Bhide PG, Young AB, Penney J, Vonsattel JP, Aronin N, DiFiglia M. (1997) Huntingtin localization in brains of normal and Huntington's disease patients. Ann Neurol. Oct;42(4):604-12.
26. Nasir J, Floresco SB, O'Kusky JR, Diewert VM, Richman JM, Zeisler J, Borowski A, Marth JD, Phillips AG, Hayden MR. (1995) Targeted disruption of the Huntington's disease gene results in embryonic lethality and behavioral and morphological changes in heterozygotes. Cell. Jun 2;81(5):811-23.

27. Imarisio S, Carmichael J, Korolchuk V, Chen CW, Saiki S, Rose C, Krishna G, Davies JE, Ttofi E, Underwood BR, Rubinsztein DC. (2008) Huntington's disease: from pathology and genetics to potential therapies. Biochem J. Jun 1;412(2):191-209.
28. Walker FO. (2007) Huntington's Disease. Semin Neurol. Apr;27(2):143-50.
29. Sugars KL, Rubinsztein DC. (2003) Transcriptional abnormalities in Huntington disease. Trends Genet. May;19(5):233-8.
30. Bano D, Zanetti F, Mende Y, Nicotera P. (2011) Neurodegenerative processes in Huntington's disease. Cell Death Dis. Nov 10;2:e228.
31. Sieradzan KA, Mechan AO, Jones L, Wanker EE, Nukina N, Mann DM. (1999) Huntington's disease intranuclear inclusions contain truncated, ubiquitinated huntingtin protein. Exp Neurol. Mar;156(1):92-9.
32. Wellington CL, Ellerby LM, Gutekunst CA, Rogers D, Warby S, Graham RK, Loubser O, van Raamsdonk J, Singaraja R, Yang YZ, Gafni J, Bredesen D, Hersch SM, Leavitt BR, Roy S, Nicholson DW, Hayden MR. (2002) Caspase cleavage of mutant huntingtin precedes neurodegeneration in Huntington's disease. J Neurosci. Sep 15;22(18):7862-72.
33. Graham RK, Deng Y, Slow EJ, Haigh B, Bissada N, Lu G, Pearson J, Shehadeh J, Bertram L, Murphy Z, Warby SC, Doty CN, Roy S, Wellington CL, Leavitt BR, Raymond LA, Nicholson DW, Hayden MR. (2006) Cleavage at the caspase-6 site is required for neuronal dysfunction and degeneration due to mutant huntingtin. Cell. Jun 16;125(6):1179-91.
34. Ratovitski T, Nakamura M, D'Ambola J, Chighladze E, Liang Y, Wang W, Graham R, Hayden MR, Borchelt DR, Hirschhorn RR, Ross CA. (2007) N-terminal proteolysis of full-length mutant huntingtin in an inducible PC12 cell model of Huntington's disease. Cell Cycle. Dec 1;6(23):2970-81.
35. Ratovitski T, Gucek M, Jiang H, Chighladze E, Waldron E, D'Ambola J, Hou Z, Liang Y, Poirier MA, Hirschhorn RR, Graham R, Hayden MR, Cole RN, Ross CA. (2009) Mutant huntingtin N-terminal fragments of specific size mediate aggregation and toxicity in neuronal cells. J Biol Chem. Apr 17;284(16):10855-67.
36. Ross CA. (2002) Polyglutamine pathogenesis: emergence of unifying mechanisms for Huntington's disease and related disorders. Neuron. Aug 29;35(5):819-22.
37. Arrasate M, Mitra S, Schweitzer ES, Segal MR, Finkbeiner S. (2004) Inclusion body formation reduces levels of mutant huntingtin and the risk of neuronal death. Nature. Oct 14;431(7010):805-1.

38. Zheng Z, Diamond MI. Huntington disease and the huntingtin protein. (2012) Prog Mol Biol Transl Sci. ;107:189-214.
39. Dunah AW, Jeong H, Griffin A, Kim YM, Standaert DG, Hersch SM, Mouradian MM, Young AB, Tanese N, Krainc D. (2002) Sp1 and TAFII130 transcriptional activity disrupted in early Huntington's disease. Science. Jun 21;296(5576):2238-43.
40. Ravache M, Weber C, Mérienne K, Trottier Y. (2010) Transcriptional activation of REST by Sp1 in Huntington's disease models. PLoS One. Dec 14;5(12):e14311.
41. Steffan JS, Bodai L, Pallos J, Poelman M, McCampbell A, Apostol BL, Kazantsev A, Schmidt E, Zhu YZ, Greenwald M, Kurokawa R, Housman DE, Jackson GR, Marsh JL, Thompson LM. (2001) Histone deacetylase inhibitors arrest polyglutamine-dependent neurodegeneration in Drosophila. Nature. Oct 18;413(6857):739-43.
42. Zuccato C, Ciammola A, Rigamonti D, Leavitt BR, Goffredo D, Conti L, MacDonald ME, Friedlander RM, Silani V, Hayden MR, Timmusk T, Sipione S, Cattaneo E. (2001) Loss of huntingtin-mediated BDNF gene transcription in Huntington's disease. Science. Jul 20;293(5529):493-8.
43. Luthi-Carter R, Strand A, Peters NL, Solano SM, Hollingsworth ZR, Menon AS, Frey AS, Spektor BS, Penney EB, Schilling G, Ross CA, Borchelt DR, Tapscott SJ, Young AB, Cha JH, Olson JM. (2000) Decreased expression of striatal signaling genes in a mouse model of Huntington's disease. Hum Mol Genet. May 22;9(9):1259-71.
44. Nucifora FC Jr, Sasaki M, Peters MF, Huang H, Cooper JK, Yamada M, Takahashi H, Tsuji S, Troncoso J, Dawson VL, Dawson TM, Ross CA. (2001) Interference by huntingtin and atrophin-1 with cbp-mediated transcription leading to cellular toxicity. Science. Mar 23;291(5512):2423-8.
45. Wyttenbach A, Swartz J, Kita H, Thykjaer T, Carmichael J, Bradley J, Brown R, Maxwell M, Schapira A, Orntoft TF, Kato K, Rubinsztein DC. (2001) Polyglutamine expansions cause decreased CRE-mediated transcription and early gene expression changes prior to cell death in an inducible cell model of Huntington's disease. Hum Mol Genet. Aug 15;10(17):1829-45.
46. Sipione S, Rigamonti D, Valenza M, Zuccato C, Conti L, Pritchard J, Kooperberg C, Olson JM, Cattaneo E. (2002) Early transcriptional profiles in huntingtin-inducible striatal cells by microarray analyses. Hum Mol Genet. Aug 15;11(17):1953-65.

47. Chen CM. (2011) Mitochondrial dysfunction, metabolic deficits, and increased oxidative stress in Huntington's disease. Chang Gung Med J. Mar-Apr;34(2):135-52.
48. Jin YN, Johnson GV. (2010) The interrelationship between mitochondrial dysfunction and transcriptional dysregulation in Huntington disease. J Bioenerg Biomembr. Jun;42(3):199-205.
49. Raymond LA, André VM, Cepeda C, Gladding CM, Milnerwood AJ, Levine MS. (2011) Pathophysiology of Huntington's disease: time-dependent alterations in synaptic and receptor function. Neuroscience. Dec 15;198:252-73.
50. Faideau M, Kim J, Cormier K, Gilmore R, Welch M, Auregan G, Dufour N, Guillermier M, Brouillet E, Hantraye P, Déglon N, Ferrante RJ, Bonvento G. (2010) In vivo expression of polyglutamine-expanded huntingtin by mouse striatal astrocytes impairs glutamate transport: a correlation with Huntington's disease subjects. Hum Mol Genet. Aug 1;19(15):3053-67.
51. Bradford J, Shin JY, Roberts M, Wang CE, Sheng G, Li S, Li XJ. (2010) Mutant huntingtin in glial cells exacerbates neurological symptoms of Huntington disease mice. J Biol Chem. Apr 2;285(14):10653-61.
52. Hassel B, Tessler S, Faull RL, Emson PC. (2008) Glutamate uptake is reduced in prefrontal cortex in Huntington's disease. Neurochem Res. Feb;33(2):232-7.
53. Liévens JC, Woodman B, Mahal A, Spasic-Boscovic O, Samuel D, Kerkerian-Le Goff L, Bates GP. (2001) Impaired glutamate uptake in the R6 Huntington's disease transgenic mice. Neurobiol Dis. Oct;8(5):807-21.
54. Milnerwood AJ, Gladding CM, Pouladi MA, Kaufman AM, Hines RM, Boyd JD, Ko RW, Vasuta OC, Graham RK, Hayden MR, Murphy TH, Raymond LA. (2010) Early increase in extrasynaptic NMDA receptor signaling and expression contributes to phenotype onset in Huntington's disease mice. Neuron. Jan 28;65(2):178-90.
55. Zeron MM, Fernandes HB, Krebs C, Shehadeh J, Wellington CL, Leavitt BR, Baimbridge KG, Hayden MR, Raymond LA. (2004) Potentiation of NMDA receptor-mediated excitotoxicity linked with intrinsic apoptotic pathway in YAC transgenic mouse model of Huntington's disease. Mol Cell Neurosci. Mar;25(3):469-79.
56. Okamoto S, Pouladi MA, Talantova M, Yao D, Xia P, Ehrnhoefer DE, Zaidi R, Clemente A, Kaul M, Graham RK, Zhang D, Vincent Chen HS, Tong G, Hayden MR, Lipton SA. (2009) Balance between synaptic versus extrasynaptic NMDA receptor activity influences inclusions and neurotoxicity of mutant huntingtin. Nat Med. Dec;15(12):1407-13.

57. Mangiarini L, Sathasivam K, Seller M, Cozens B, Harper A, Hetherington C, Lawton M, Trottier Y, Lehrach H, Davies SW, Bates GP. (1996) Exon 1 of the HD gene with an expanded CAG repeat is sufficient to cause a progressive neurological phenotype in transgenic mice. Cell 87:493-506.
58. Hodgson JG, Agopyan N, Gutekunst CA, Leavitt BR, LePiane F, Singaraja R, Smith DJ, Bissada N, McCutcheon K, Nasir J, Jamot L, Li XJ, Stevens ME, Rosemond E, Roder JC, Phillips AG, Rubin EM, Hersch SM, Hayden MR. (1999) A YAC mouse model for Huntington's disease with full-length mutant huntingtin, cytoplasmic toxicity, and selective striatal neurodegeneration. Neuron 23:181-192.
59. Wenk MR. (2005) The emerging field of lipidomics. Nat Rev Drug Discov. Jul;4(7):594-610.
60. Fahy E, Subramaniam S, Brown HA, Glass CK, Merrill AH Jr, Murphy RC, Raetz CR, Russell DW, Seyama Y, Shaw W, Shimizu T, Spener F, van Meer G, VanNieuwenhze MS, White SH, Witztum JL, Dennis EA. (2005) A comprehensive classification system for lipids. J Lipid Res. May;46(5):839-61.
61. Dietschy JM, Turley SD. (2004) Thematic review series: brain Lipids. Cholesterol metabolism in the central nervous system during early development and in the mature animal. J Lipid Res.Aug;45(8):1375-97.
62. Adibhatla RM, Hatcher JF. (2007) Role of Lipids in Brain Injury and Diseases. Future Lipidol. Aug;2(4):403-422.
63. Björkhem I, Meaney S. (2004) Brain cholesterol: long secret life behind a barrier. Arterioscler Thromb Vasc Biol. May;24(5):806-15.
64. Edwards PA, Lan SF, Tanaka RD, Fogelman AM. (1983) Mevalonolactone inhibits the rate of synthesis and enhances the rate of degradation of 3-hydroxy-3-methylglutaryl coenzyme A reductase in rat hepatocytes. J Biol Chem. Jun 25;258(12):7272-5.
65. Chun KT, Bar-Nun S, Simoni RD. (1990) The regulated degradation of 3-hydroxy-3-methylglutaryl-CoA reductase requires a short-lived protein and occurs in the endoplasmic reticulum. J Biol Chem. Dec 15;265(35):22004-10.
66. Goldstein JL, Brown MS. (1990) Regulation of the mevalonate pathway. Nature. Feb 1;343(6257):425-30.
67. Brown MS, Goldstein JL. (1997) The SREBP pathway: regulation of cholesterol metabolism by proteolysis of a membrane-bound transcription factor. Cell. May 2;89(3):331-40.

68. Horton JD, Shimomura I. (1999) Sterol regulatory element-binding proteins: activators of cholesterol and fatty acid biosynthesis. Curr Opin Lipidol. Apr;10(2):143-50.
69. Sakakura Y, Shimano H, Sone H, Takahashi A, Inoue N, Toyoshima H, Suzuki S, Yamada N. (2001) Sterol regulatory element-binding proteins induce an entire pathway of cholesterol synthesis. Biochem Biophys Res Commun. Aug 10;286(1):176-83.
70. Pfrieger FW. (2003) Outsourcing in the brain: do neurons depend on cholesterol delivery by astrocytes? Bioessays. Jan;25(1):72-8.
71. Vance JE, Pan D, Campenot RB, Bussière M, Vance DE. (1994) Evidence that the major membrane lipids, except cholesterol, are made in axons of cultured rat sympathetic neurons. J Neurochem. Jan;62(1):329-37.
72. Chintagari NR, Jin N, Wang P, Narasaraju TA, Chen J, Liu L. (2006) Effect of cholesterol depletion on exocytosis of alveolar type II cells. Am J Respir Cell Mol Biol. Jun;34(6):677-87.
73. Guo J, Chi S, Xu H, Jin G, Qi Z. (2008) Effects of cholesterol levels on the excitability of rat hippocampal neurons. Mol Membr Biol. Apr;25(3):216-23.
74. Lütjohann D. (2006) Cholesterol metabolism in the brain: importance of 24S-hydroxylation. Acta Neurol Scand Suppl. 185:33-42.
75. Ikonen E. (2006) Mechanisms for cellular cholesterol transport: defects and human disease. Physiol Rev. Oct;86(4):1237-61.
76. DeBarber AE, Eroglu Y, Merkens LS, Pappu AS, Steiner RD. (2011) Smith-Lemli-Opitz syndrome. Expert Rev Mol Med. Jul 22;13:e24.
77. Porter FD, Herman GE. (2011) Malformation syndromes caused by disorders of cholesterol synthesis. J Lipid Res. Jan;52(1):6-34.
78. Liu JP, Tang Y, Zhou S, Toh BH, McLean C, Li H. (2010) Cholesterol involvement in the pathogenesis of neurodegenerative diseases. Mol Cell Neurosci. Jan;43(1):33-42.
79. Valenza M, Rigamonti D, Goffredo D, Zuccato C, Fenu S, Jamot L, Strand A, Tarditi A, Woodman B, Racchi M, Mariotti C, Di Donato S, Corsini A, Bates G, Pruss R, Olson JM, Sipione S, Tartari M, Cattaneo E. (2005) Dysfunction of the cholesterol biosynthetic pathway in Huntington's disease. J Neurosci. Oct 26;25(43):9932-9.
80. Valenza M, Cattaneo E. (2006) Cholesterol dysfunction in neurodegenerative diseases: is Huntington's disease in the list? Prog Neurobiol. Nov;80(4):165-76.
81. Briggs MR, Yokoyama C, Wang X, Brown MS, Goldstein JL. (1993) Nuclear protein that binds sterol regulatory element of low density lipoprotein receptor

promoter. I. Identification of the protein and delineation of its target nucleotide sequence. J Biol Chem. Jul 5;268(19):14490-6.

82. Wang X, Briggs MR, Hua X, Yokoyama C, Goldstein JL, Brown MS. (1993) Nuclear protein that binds sterol regulatory element of low density lipoprotein receptor promoter. II. Purification and characterization. J Biol Chem. Jul 5;268(19):14497-504.
83. Brown MS, Goldstein JL. (1997) The SREBP pathway: regulation of cholesterol metabolism by proteolysis of a membrane-bound transcription factor. Cell. May 2;89(3):331-40.
84. Horton JD. Sterol regulatory element-binding proteins: transcriptional activators of lipid synthesis. (2002) Biochem Soc Trans. Nov;30(Pt 6):1091-5.
85. Fahrenkrog B & Aebi U. The nuclear pore complex: nucleocytoplasmic transport and beyond. (2003) Nature Reviews Molecular Cell Biology 4, 757-766
86. Bonner, W. M. 1978. Protein migration and accumulation in nuclei. In The Cell Nucleus. H. Bush, editor. Academic Press, Inc., New York. 97-148.
87. Radu A, Blobel , Mooret MS. (1975) Identification of a protein complex that is required for nuclear protein import and mediates docking of import substrate to distinct nucleoporins (1975) Proc. Natl. Acad. Sci. USA Vol. 92, pp. 1769-1773.
88. Gorlich D, Prehn S,Laskey RA , Hartmann E. (1994) Isolation of a protein that is essential for the first step of nuclear protein import. Cell, 79:767-778.
89. Stade, K, Ford, C S, Guthrie, C, and Weis, K. (1997) Exportin 1 (Crm1p) is an essential nuclear export factor. Cell. 90(6), 1041-1050.
90. Cingolani G, Petosa C, Weis K, Müller CW. (1999) Structure of importin-beta bound to the IBB domain of importin-alpha. Nature. May 20;399(6733):221-9

Gorlich D. (1997). Nuclear protein import. Curr. Opin. Cell Biol. 9, 412–419.

92. Görlich D, Kostka S, Kraft R, Dingwall C, Laskey RA, Hartmann E, Prehn S. (1995) Two different subunits of importin cooperate to recognize nuclear localization signals and bind them to the nuclear envelope. Curr Biol. Apr 1;5(4):383-92.

Lee SJ, Matsuura Y, Liu SM & Stewart M. (2005) Structural basis for nuclear import complex disassembly by RanGTP. Nature, 435:693-696.

Forwood JK, Lam MH, Jans DA. (2001) Nuclear import of Creb and AP-1 transcription factors requires importin-beta 1 and Ran but is independent of importin-alpha. Biochemistry. May 1;40(17):5208-17.

95. Chen X, Xu L. Mechanism and regulation of nucleocytoplasmic trafficking of smad. (2011) Cell Biosci. Dec 28;1.

96. Yu RK, Nakatani Y, Yanagisawa M. (2009) The role of glycosphingolipid metabolism in the developing brain. J Lipid Res. Apr;50 Suppl:S440-5.
97. Gulati S, Liu Y, Munkacsi AB, Wilcox L, Sturley SL. (2010) Sterols and sphingolipids: dynamic duo or partners in crime? Prog Lipid Res. Oct;49(4):353-65.
98. Ichikawa N, Iwabuchi K, Kurihara H, Ishii K, Kobayashi T, Sasaki T, Hattori N, Mizuno Y, Hozumi K, Yamada Y, Arikawa-Hirasawa E. (2009) Binding of laminin-1 to monosialoganglioside GM1 in lipid rafts is crucial for neurite outgrowth. J Cell Sci. Jan 15;122(Pt 2):289-99.
99. Sonnino S, Mauri L, Chigorno V, Prinetti A. (2007) Gangliosides as components of lipid membrane domains. Glycobiology. Jan;17(1):1R-13R.
100. Posse de Chaves E, Sipione S. (2010) Sphingolipids and gangliosides of the nervous system in membrane function and dysfunction. FEBS Lett. May 3;584(9):1748-59.
101. Ngamukote S, Yanagisawa M, Ariga T, Ando S, Yu RK. (2007) Developmental changes of glycosphingolipids and expression of glycogenes in mouse brains. J Neurochem. Dec;103(6):2327-41.
102. Svennerholm L, Boström K, Fredman P, Månsson JE, Rosengren B, Rynmark BM. (1989) Human brain gangliosides: developmental changes from early fetal stage to advanced age. Biochim Biophys Acta. Sep 25;1005(2):109-17.
103. Fishman PH, Max SR, Tallman JF, Brady RO, Maclaren NK, Cornblath M. (1975) Deficient Ganglioside Biosynthesis: a novel human sphingolipidosis. Science. Jan 10;187(4171):68-70.
104. Simpson MA, Cross H, Proukakis C, Priestman DA, Neville DC, Reinkensmeier G, Wang H, Wiznitzer M, Gurtz K, Verganelaki A, Pryde A, Patton MA, Dwek RA, Butters TD, Platt FM, Crosby AH. (2004) Infantile-onset symptomatic epilepsy syndrome caused by a homozygous loss-of-function mutation of GM3 synthase. Nat Genet. Nov;36(11):1225-9.
105. Squitieri F, Frati L, Ciarmiello A, Lastoria S, Quarrell O. (2006) Juvenile Huntington's disease: does a dosage-effect pathogenic mechanism differ from the classical adult disease? Mech Ageing Dev. Feb;127(2):208-12.
106. Chan RB, Oliveira TG, Cortes EP, Honig LS, Duff KE, Small SA, Wenk MR, Shui G, Di Paolo G. (2012) Comparative lipidomic analysis of mouse and human brain with Alzheimer disease. J Biol Chem. Jan 20;287(4):2678-88.
107. Maglione V, Marchi P, Di Pardo A, Lingrell S, Horkey M, Tidmarsh E, Sipione S. (2010) Impaired ganglioside metabolism in Huntington's disease and neuroprotective role of GM1. J Neurosci. Mar 17;30(11):4072-80.

108. Valenza M, Carroll JB, Leoni V, Bertram LN, Björkhem I, Singaraja RR, Di Donato S, Lutjohann D, Hayden MR, Cattaneo E. (2007) Cholesterol biosynthesis pathway is disturbed in YAC128 mice and is modulated by huntingtin mutation. Hum Mol Genet. Sep 15;16(18):2187-98.
109. Valenza M, Leoni V, Tarditi A, Mariotti C, Björkhem I, Di Donato S, Cattaneo E. (2007) Progressive dysfunction of the cholesterol biosynthesis pathway in the R6/2 mouse model of Huntington's disease. Neurobiol Dis. Oct;28(1):133-42.
110. Valenza M, Leoni V, Karasinska JM, Petricca L, Fan J, Carroll J, Pouladi MA, Fossale E, Nguyen HP, Riess O, MacDonald M, Wellington C, DiDonato S, Hayden M, Cattaneo E. (2010) Cholesterol defect is marked across multiple rodent models of Huntington's disease and is manifest in astrocytes. J Neurosci. Aug 11;30(32):10844-50.
111. Higatsberger MR, Sperk G, Bernheimer H, Shannak KS, Hornykiewicz O. (1981) Striatal ganglioside levels in the rat following kainic acid lesions: comparison with Huntington's disease. Exp Brain Res. ;44(1):93-6.
112. Desplats PA, Denny CA, Kass KE, Gilmartin T, Head SR, Sutcliffe JG, Seyfried TN, Thomas EA. (2007) Glycolipid and ganglioside metabolism imbalances in Huntington's disease. Neurobiol Dis. Sep;27(3):265-77.
113. Ferrari G, Anderson BL, Stephens RM, Kaplan DR, Greene LA. (1995) Prevention of apoptotic neuronal death by GM1 ganglioside. Involvement of Trk neurotrophin receptors. J Biol Chem. Feb 17;270(7):3074-80.
114. Wu G, Lu ZH, Xie X, Ledeen RW. (2004) Susceptibility of cerebellar granule neurons from GM2/GD2 synthase-null mice to apoptosis induced by glutamate excitotoxicity and elevated KCl: rescue by GM1 and LIGA20. Glycoconj J. ;21(6):305-13.
115. Pope-Coleman A, Tinker JP, Schneider JS. (2000) Effects of GM1 ganglioside treatment on pre- and postsynaptic dopaminergic markers in the striatum of parkinsonian monkeys. Synapse. May;36(2):120-8.
116. Oppenheimer S. (1990) GM1 ganglioside therapy in acute ischemic stroke. Stroke. May;21(5):825.

2. CHAPTER 1

DYSREGULATION OF THE CHOLESTEROL BIOSYNTHETIC PATHWAY IN HD

Mutant Huntingtin interacts with the transcription factor SREBP and impairs its nuclear translocation.

2.1. INTRODUCTION

Recent findings suggest that dysregulation of cholesterol synthesis occurs in HD (1-4). Brain cholesterol, almost all locally synthesized, plays a critical role in the regulation of neuronal functions and in the maintenance of CNS homeostasis (5). Cholesterol biosynthesis is tightly regulated by membrane-bound transcription factors known as sterol regulatory element binding proteins (SREBPs), normally located as inactive precursor proteins in the membrane of the endoplasmic reticulum (ER) (6) In humans, three different SREBP proteins with different role in lipid metabolism are expressed: SREBP1a, SREBP1c and SREBP2.

Both SREBP1a and 1c are produced from a single gene through the use of alternative transcription sites (7), while SREBP2 is transcribed from a separate gene (8). SREBP1a is a potent activator of all SREBP-responsive genes, including those that mediate the synthesis of cholesterol, fatty acids, and triglycerides. SREBP1c regulates the transcription of genes required for fatty acids, but not cholesterol synthesis. Finally, SREBP2 is specifically involved in the activation of cholesterol biosynthesis (9).

SREBP-2 is synthesized as a large, transcriptionally inactive precursor localized in the endoplasmic reticulum (ER). When cholesterol levels are low, SREBP2 translocates from the ER to the Golgi apparatus through binding to an escort protein named SREBP cleavage activation protein (SCAP), a process that is blocked under cholesterol excess by insulin-induced gene 1 (INSIG1) and insulin-induced gene 2 (INSIG2) proteins (10, 11). Once in the Golgi, SREBP-2 undergoes specific proteolytic

cleavage by two membrane-associated proteases, the site 1 (S1P) and site 2 (S2P) proteases, which yields an active 68-kDa N-terminal fragment (mature SREBP-2, mSREBP-2) that translocates to the nucleus, together with the nuclear transporter importin-beta, binds the sterol response element (SRE) in the promoters of target cholesterogenic genes (Figure 1.5) and activates their transcription. The subsequent accumulation of sterols in ER membranes prevents further proteolytic activation of SREBP-2 by blocking the exit of SCAP-SREBP-2 complex from the ER; transcription of SREBP-2 target genes decline and cholesterol synthesis and uptake are suppressed.

The possibility that changes in cholesterol homeostasis occur in HD has received substantial attention from many investigators over the past several years. MHtt has been shown to induce down-regulation of the expression of the genes involved in the cholesterol biosynthetic pathway in HD cell models (13), in HD transgenic mouse models and in human post-mortem brains (1,2,4,).

Although alterations in cholesterol content have been widely described across multiple HD models, little is know about the underlying molecular mechanism. Our previous data suggested that altered cholesterol biosynthesis in HD is attributable to decreased presence of mSREBP2 in the nucleus (1). However, how mHtt might affect the SREBP2 pathway, remains to be determined. In this study we explored the possibility that mHtt might physically interact with mSREBP2 and impair its translocation into the nucleus. In support of this hypothesis, we showed that mHtt retains the complex SREBP2/importin-! in the cytoplasm of HD cells, therefore reducing mSREBP2 availability in the nucleus and ultimately impairing its regulatory activity on cholesterogenic gene transcription.

2.2. MATERIAL AND METHODS

2.2.1. Animal and cell models

YAC128 mice were purchased from the Jackson Laboratories (Jackson Laboratories, Bar Harbor, ME, USA). Female YAC128 mice were crossed with male FVB/N wild-type mice for colony maintenance. All procedures on animals were approved by the University of Alberta's Animal Care and Use Committee and were in accordance with the guidelines of the Canadian Council on Animal Care. Conditionally-immortalized rat striatal ST14A cells and ST14A cells expressing an N-terminal fragment of mHtt containing 120 glutamines (N548-120Q) were kindly provided by Dr. E. Cattaneo (University of Milan, Italy) and maintained in culture at the permissive temperature (33ºC) as previously reported (12). Conditionally-immortalized mouse striatal knock-in cells expressing endogenous levels of wild-type (ST*Hdh*$^{7/7}$) or mHtt (ST*Hdh*$^{111/111}$) were a gift from Dr. M.E. MacDonald (Massachusetts General Hospital, Boston, MA, USA) and were maintained as previously described (12). Human skin fibroblasts isolated from HD patients (line GM03621, expressing one *HD* allele with 61 CAG repeats) were purchased from Coriell Cell Repositories (Coriell Institute for Medical Research, Camden, NJ, USA) and grown in modified Eagle's Medium (MEM, Invitrogen) supplemented with 15% fetal bovine serum (FBS), 2 mM L-glutamine, 100 U/mL penicillin, 100 $g/mL streptomycin and 0.11 g/L sodium pyruvate. Primary neuronal cultures were obtained from cerebral cortex and striatum of newborn mice (P0). Briefly, after dissection cerebral cortex and striatum were minced and digested with 1 mg/ml papain for 10 min at 37°C. DNase was added to the digestion mix in the last 5 min of incubation. Cells were centrifuged at 200 x *g* for 1 min, resuspended in Neurobasal-A medium (Invitrogen) supplemented with 1% B27 (Invitrogen), and gently dissociated by pipetting up and down. Neurons were plated onto poly-D-lysine-coated

wells at a density of 1 X 10^5 cells/cm^2 and used for experiments at 9–11 d *in vitro* (DIV).

2.2.1. Generation of mSREBP2-EGFP constructs

The cDNA for the mature form of human SREBP2 (aa. 1-484) was cloned by RT-PCR from HeLa cells, the most widely used continuous cell line derived from human cervical cancer, using the following primers:

Fw: 5'-AAACTCGAGCAATGGACGACAGCGGC-3';

Rev: 5' GGGATCCTCACAGAAGAATCCGTGAGCG-3'.

The forward primer included an Xho I restriction site upstream of SREBP2 start codon, while the reverse primers included a stop codon downstream to aminoacid 484 in the human SREBP2 protein sequence (S2P cleavage site), and BamH1 restriction site for in-frame directional cloning into pEGFP-C1 vector (Clontech). The resulting pEGFP-C1-EGFP plasmid (herein referred to as EGFP-SREBP) was sequenced to verify the absence of mutations in the SREBP2 cDNA and cloning in frame with EGFP.

2.2.2. RNA extraction and real-time PCR analysis of gene expression

Total RNA from WT and YAC128 mice brain and from human fibroblasts derived from control and HD patients was extracted using RNeasy kit (Qiagen) according to the manufacturer's instructions. All RNA samples were subjected to in-column treatment with DNaseI (Qiagen) to eliminate genomic DNA contamination. One mg of total RNA was reverse-transcribed using Superscript II reverse transcriptase (Invitrogen) and oligo-d(T) primer, and the resulting cDNAs were amplified using Power SYBR® Green PCR Master Mix (Applied Biosystems, Foster City, CA), following manufacturers' instructions. Quantitative PCR analysis was carried out on a StepOnePlus™ instrument (Applied Biosystems, Foster

City, CA), by comparison with a standard curve generated by cDNA serial dilutions. Gene-specific primers were designed using Primer Express 3.0 software (Applied Biosystems, Foster City, CA, USA). The level of each mRNA was normalized to that of cyclophilin A. PCR cycling parameters were: 50°C for 2 min, 95°C for 5 min, followed by 40 cycles of 95°C for 20 sec, 60°C for 1 min and 72°C for 40 sec. Primer sequences were: Fw 5' TCC AAA GAC AGC AGA AAA CTT TCG 3', Rev 5' TCT TCT TGC TGG TCT TGC CAT TCC 3'.

2.2.3. Subcellular fractionation

Twenty-five g/ml N-acetyl-leucyl-leucyl-norleucinal (ALLN) was added to ST14A cells 2 h before lysis. Cells and fresh brain tissues from WT and YAC128 mice were homogenized in buffer A (10mM HEPES-K^+ pH7.5, 250mM sucrose, 10mM KCl, 1.5mM $MgCl_2$, 1mM EDTA, 1mM EGTA and Protease-Inhibitor Cocktail (SIGMA-Aldrich, St. Louis, MO, USA) by passing the cells 20 times through a 26-G needle. Cell lysates were incubated on ice for 20 min and then centrifuged at 1000 x g for 5 min. The supernatant (cytoplasmic fraction) was harvested and stored at –80°C until used. The nuclear pellet was washed once with buffer A and then resuspended in buffer B (20mM HEPES-K^+ pH7.9, 420mM NaCl, 0.2mM EDTA, 1.5mM $MgCl_2$, 0.5 DTT, 25% glycerol) and incubated for 1h at 4°C on a shaker. Following centrifugation at max speed of 14,500 rpm for 1h at 4°C, the supernatant (nuclear extract) was collected and stored at –80°C until used.

2.2.4. Immunoprecipitation

Immunoprecipitation of transfected EGFP-mSREBP2 was performed from cytoplasmic (0.8mg) and nuclear (0.4mg) subcellular fractions, using goat anti-EGFP antibodies (a gift from Dr. Luc Berthiaume). Huntingtin

was immunoprecipitated from cytoplasmic fractions from WT and YAC128 mouse brain using anti-Htt antibodies Ab2166 and Ab2168 in combination. Antibodies were complexed with protein G-Sepharose beads (Zymed, Invitrogen) overnight at 4°C, before incubation with cytoplasmic or nuclear fractions for 4 h at r.t. Immunoprecipitated complexes were resolved on SDS-PAGE and detected by immunoblotting with anti-Htt (mAb2166 1:5000, Chemicon), anti-EGFP and anti-SREBP2 (1:1000, AbCam) antibodies.

2.2.5. Immunoblotting

Thirty micrograms of total, cytoplasmic and nuclear proteins were resolved onto 10 % SDS-PAGE and transferred to nitrocellulose membranes (Bio-Rad Laboratories, Hercules, CA, USA). Membranes were blocked with 5% non-fat milk in TBS-T buffer, for 1 h at room temperature and then incubated overnight at 4°C with the primary antibodies: anti-SREBP2 (rabbit polyclonal antibody 1:1000, AbCam), anti beta-tubulin (mouse monoclonal antibody 1:1000 Cell Signaling), anti Histone 1 (rabbit polyclonal antibody 1:1000 Santa Cruz) or anti Lamin A/C (rabbit polyclonal antibody 1:1000 Cell Signaling). After washing, incubation with HRP-conjugated secondary antibodies was performed for 1h at room temperature. Detection was performed using ECL Plus (Amersham Biosciences) chemiluminescence reagents. Densitometric analysis was performed using Quantity One® software (Bio-Rad Laboratories, Hercules, CA, USA).

2.2.6. Detection of mHtt aggregates and filter-trap assay

Cell lysates from wild-type and HD cells transfected with EGFP-mSREBP2 were prepared as described. Thirty ug of total or cytoplasmic cellular proteins were resolved on 6% SDS-PAGE and both stacking and

resolving gel were transferred to a nitrocellulose membrane (Bio-Rad Laboratories, Hercules, CA, USA) for immunoblotting. SDS-insoluble mHtt aggregates were detected in the stacking gel by immunoblotting with the rabbit polyclonal antibody EM48 (Chemicon). To detect EGFP-mSREBP2, goat anti-GFP antibodies were used (a gift from Dr. Luc Berthiaume, University of Alberta). To perform the filter trap assay, cytoplasmic cell fractions were centrifuged at 13,000 x *g* for 10 min. The resulting pellet was resuspended in 2% SDS, incubated for 15 min at room temperature and sonicated for 10 s, before being filtered through a cellulose acetate membrane (Schleicher and Schuell, 0.2-$m pore size), using a dot-blot filtration unit (BioRad). The membrane was washed with PBS + 1% SDS. SDS-insoluble aggregates retained on the membrane were detected with anti-Htt antibodies (mAB2166, 1:1000, Chemicon) followed by incubation with anti-mouse-HRP antibodies (1:10,000, BioRad) and ECL chemiluminescence (Amersham Biosciences, Inc.).

2.2.7. Cell transfection

Rat and mouse striatal cell lines were transiently transfected with EGFP-mSREBP2 or EGFP alone using Lipofectamine 2000 (Invitrogen) according to the manufacturer's instructions. Primary cortical and striatal neurons were transfected prior to plating, using the Mouse Neurons Nucleofector Kit (Amaxa Biosystems Inc.) according to the manufacturer's instructions. Briefly, 2 % 10^6 neurons were suspended in 100 l of Nucleofector reagent and 1 g of plasmid was added for nucleofection. Electroporated neurons were immediately plated on coverslips previously coated with poly-L-lysine, and cultured for 36 h at 37°C before confocal microscopy analysis.

2.2.8. Immunocytochemistry and confocal microscopy

Twenty-four to thirty-six hours after transfection with the indicated plasmids, cells were washed in Dulbecco's phosphate buffered saline (PBS), fixed in 4% paraformaldehyde for 10min at room temperature and permeabilized with 0.5% Triton-X-100 in PBS for 5 min. After blocking with 4% donkey serum for 1 h at room temperature, cells were incubated with anti-Htt antibodies: mAb2166 (1:500, Chemicon) or EM48 (1:500, Chemicon), followed by Alexa 555-conjugated donkey anti mouse antibodies (1:500, Molecular Probes). Nuclei were counterstained with 4',6-diamidino-2-phenylindole (DAPI, Vector Laboratories, Burlingame, CA) for10 min at room temperature). Coverslips were mounted using ProLong Gold antifade reagent (Molecular Probes). Slides were analyzed with an LSM510 laser scanning confocal microscope mounted on a Zeiss Axiovert 100M microscope, using a 63X oil immersion lens. Images for wild-type and HD cells were acquired using the same confocal settings. A minimum of 100 cells were analysed to determine the percentage of cells with cytoplasmic localization of EGFP-mSREBP2. Analysis of colocalization was performed using ZEN 2009 software (Carl Zeiss Mikroskopie, German).

2.2.9. Transfection in cortical neurons

Dissociated cortical neurons were transfected using the mouse Neuron Nucleofector kit available from Amaxa Biosystems, Inc. Following dissociation, approximately four million cells were pelleted and re-suspended in 100 l of mouse Nucleofector Solution containing 2 g of eGFP-hnSREBP2 plasmid. The neuron/Nucleofector suspension was transferred to a sterile cuvette and electroporated by using program 0-005. 500 l of warmed neuron growth media was added to the cell suspension and cells were then immediately plated on coverslips and cultured for 48 hrs at 37°C.

2.2.10. Statistical Analysis

All the data are expressed as the mean +/- standard deviation. Statistical analysis was performed using the two-tail *t* test (Prism 4.0 software, GraphPad). A cut-off value of $p<0.05$ was used for statistical significance.

2.3. RESULTS

2.3.1. Altered subcellular distribution of mature SREBP2 in cortical tissue from YAC128 mice

Levels of SREBP2 precursor (pSREBP2) protein (Figure 2.1A) and cleaved (mature) SREBP-2 (mSREBP-2, Figure 2.1B) in total lysates from cortex and striatum were comparable between 6 month-old YAC128 mice and WT littermates. However, following subcellular fractionation of cortical tissue, we observed a partial but significant redistribution of mSREBP2 from the nuclear to the cytoplasmic fraction of YAC128 mice (Figure 2.1B). This suggested that, in spite of normal SREBP2 processing, nuclear localization of mSREBP2 is affected in the cerebral cortex of HD mice. Partitioning of mSREBP2 between cytoplasmic and nuclear fractions was not affected in the striatum of 6 month-old YAC128 mice compared to controls (Figure 2.1B). In agreement with these findings, expression of two SREBP2-responsive genes, SREBP2 and HMGCR, was decreased in the cortex, but not in the striatum of 6 month-old YAC128 mice (Figure 2.1C). However, SREBP2-dependent transcription was found to be affected in the striatum of older YAC128 mice (Figure 2.2), suggesting that SREBP2 nuclear translocation might be affected in the cortex earlier than in the striatum.

2.3.2. Aberrant intracellular localization of mSREBP2- and mSREBP1c-EGFP in cells expressing mHtt

To confirm that the intracellular localization of mSREBP2 is affected in HD cells we expressed a chimeric form of mSREBP2 fused to the fluorescente protein EGFP (mSREBP2-EGFP) in immortalized rat striatal cells (ST14A) expressing either wild-type (N548-15Q) or mutant (N548-128Q) Htt N-terminal fragments. As expected, in parental cells and in cells expressing wild-type Htt the chimeric protein was localized in the nucleus

in most of the cells (Figure 2.3A). On the contrary, in cells expressing mHtt SREBP2 was localized both in the nucleus and in the cytoplasm (Figs. 2.3A and 2.3B). Aberrant localization of the chimeric protein was also observed in other cell models of HD, including knock-in cells expressing full-length mHtt (STHdh111/111) (Figs. 2.3B and 2.3C), primary cortical YAC128 neurons (Figure 2.3D), and fibroblasts isolated from HD patients (Figs. 2.3E). Similar results were obtained after subcellular fractionation and detection of mSREBP2-EGFP in the cytoplasmic fraction of STHdh111/111 (Figure 2.3C) and N548-128Q cells (Figure 2.4). In line with the observation that mSREBP2-EGFP is mislocalized in HD cells we found that transcription of an SREBP2-responsive gene, HMG-CoA reductase, was increased to a greater extent in normal cells transfected with mSREBP2 than in HD cells transfected with the same cDNA (Figure 2.5). Similarly to mSREBP2, mSREBP1c-EGFP was also mislocalized in transfected human HD fibroblasts (Figure 2.6A) and in HD mouse striatal-derived cells (Figure 2.6B), indicating that mHtt interferes not only with the transcriptional activity of both members of the family, thus potentially affecting cholesterol as well as fatty acid metabolism. Aberrant mSREBPs localization in the cytoplasm of HD cells was not due to overall impaired nuclear transport, as shown by correct nuclear localization of EGFP containing a classic nuclear localization signal (NLS-EGFP) in HD cells (Figure 2.7).

2.3.3. mSREBP mislocalization is not due to entrapment in insoluble aggregates of mHtt

MHtt protein aggregates can bind and sequester a number of proteins and transcription factors (14). To determine whether mSREBP2 was trapped into insoluble mHtt aggregates we performed filter-trap assay after transfection of HD cells with mSREBP2-EGFP. SDS-insoluble aggregates of mHtt were retained on the acetate filter, but no mSREBP2-EGFP2 was

detectable by immunoblotting in the SDS-insoluble fraction (Figure 2.8A). Results were confirmed by SDS-PAGE and immunoblotting showing no detectable mSREBP2-EGFP in the insoluble material in the stacking gel (Figure 2.8B). Similarly, no colocalization of mSREBP2-EGFP with mHtt aggregates (detected with EM48 antibodies) was observed by confocal microscopy (Figure 2.8C).

2.3.4. mSREBP2 interacts with mHtt

Although mSREBP2 was not sequestered in insoluble aggregates with mHtt, it colocalized with soluble mHtt (Figure 2.8D). To determine whether mSREBP2 and Htt interact with each other we expressed and immunoprecipitated mSREBP2-EGFP from the cytoplasmic fraction of various HD cell model. In N548-128Q cells, N-terminal fragments of mHtt co-immunoprecipitated with mSREBP2-EGFP (Figure 2.9A). The interaction was specific for mSREBP2, as no Htt was co-immunoprecipitated from control cells expressing EGFP only (Figure 2.9A). Wild-type Htt N-terminal fragments also co-immunoprecipitated with mSREBP2-EGFP, but to a much less extent than mHtt (Figure 2.9A). Similar results were obtained using striatal cells that express full-length Htt (Figure 2.9B). When immunoprecipitation was performed from nuclear fractions, both wild-type and mHtt co-immunoprecipitated with mSREBP2-EGFP to a similar extent (Figure 2.10), suggesting that in the nucleus Htt might be part of a transcriptional complex with mSREBP2 even in normal conditions. To determine whether endogenous mSREBP2 interacts with mHtt *in vivo* we immunoprecipitated Htt from the cytoplasmic fraction of cortical brain tissue of YAC128 mice and WT littermates. As in the cell models, endogenous mSREBP2 was co-immunoprecipitated from YAC128 tissue to a much larger extent than from WT tissue (Figure 2.9C), demonstrating an aberrant interaction occurs between mHtt and

mSREBP2 *in vivo*. No Htt or mSREBP2 were immunoprecipitated using control IgG (Figure 2.9C).

2.3.5. MHtt is in a complex with and stabilizes the interaction between mSREBP2 and importin-β

Both Htt and importin-! are characterized by the presence of HEAT repeats that mediate protein-protein interactions. In the case of importin-! , one of the HEAT domains is essential for binding to mSREBP2 and transport of the transcription factor to the nucleus (15). Therefore, we hypothesized that mHtt might prevent mSREBP2 transport to the nucleus by competing with importin-! for the binding to mSREBP2. To test this hypothesis, we measured the amount of import beta that co-immunoprecipitated with mSREBP2-EGFP in cells expressing wild-type or mHtt. The expectation was that we would detect less importing beta in complex with mSREBP2-EGFP in HD cells than in control cells. To our surprise, the opposite was true. More importin-! was in complex (co-immunoprecipitated) with mSREBP2 in HD cells than in normal cells (Figure 2.11), in spite similar levels of importin-! in wild-type and HD cells (Figs. 2.11A and 2.11B). Importin-! was immunoprecipitated in complex with mHtt (both N-terminal fragments and full-length protein) and mSREBP2-EGFP (Figs. 2.11A and 2.11B), suggesting that by binding to mSREBP2, mHtt might stabilize its interaction with importin-! . Upon binding to importin-! , mSREBP2 is delivered into the nucleus. Here, binding of RanGTP to importin-! triggers the release of the cargo molecule (mSREBP2). Free importin-! diffuses back in the cytoplasm, ready to bind new cargo. Factors that interfere with this process would be expected to increase the pool of importin-! bound to mSREBP2 in the cytoplasm, as we observed in HD cells. To confirm that mHtt stabilizes the complex mSREBP2-importin-! , rather than binding importin-beta itself, we incubated the complex immunoprecipitated with anti-GFP antibodies

(recognizing the chimeric mSREBP2-EGFP) and containing mSREBP2-EGFP, mHtt and importin-! , with purified Ran GTP. As expected, binding of RanGTP to importin-! triggered the release of importin-! from the complex and into the supernatant (Figure 2.11C). However, all muHtt remained bound to mSREBP2-EGFP (Figure 2.11C), indicating that its interaction is with mSREBP2-EGFP, not directly with importin-! .

2.4. DISCUSSION

Cholesterol is an important and abundant molecule of the brain that acts as an essential structural and regulatory component of cell membranes. It is involved in numerous crucial biological processes including development of the central nervous system (CNS), transduction of cell signaling, membrane trafficking, neurotransmitter release and synaptogenesis (5). Neuronal cells rely on cholesterol for most of their activities, therefore and not surprisingly, defect in cholesterol homeostasis is likely to have a profound impact on brain functions. Abnormalities in brain cholesterol content have been associated with a number of common neurodegenerative disorders (5,16,17) including HD (1-2,13,18).

In spite of a large body of evidence showing perturbed cholesterol biosynthesis in HD models and HD patients, little is known about the underlying molecular mechanism. A previous study implicates perturbation of the SREBP2 pathway as the possible mechanism causative of altered cholesterol biosynthesis in HD (1*).* In particular*,* levels of active SREBP2 were found reduced in the nucleus of HD cells, suggesting that mHtt might mechanistically interfere with SREBP activation (1).

Processing of SREBP2 is a multistep process involving sensing of cholesterol levels by SCAP, escort of SREBP bound to SCAP from the ER and to the Golgi and proteolytic activation of the transcription factor by two different proteases proteases. Mature SREBP2 binds importin-beta and translocates to the nucleus where it activates the transcription of genes involved in the cholesterol metabolism (19). Where in this pathway mHtt affects its inhibitor activity was not known, and this study was designed to answer this question.

I found that levels of both precursor and mature form of SREBP2 protein were similar in total lysates from cortex and striatum of WT and HD mice, indicating that processing of SREBP2 was not affected in HD. However, mSREBP2 was decreased in nuclear fractions and significantly increased

in the cytoplasmic fractions of HD cerebral cortex, compared to controls. This suggested that trafficking of mSREBP2 to and localization in the nucleus might be affected by mHtt.

Nuclear translocation of SREBP2 is critical for the regulation of genes involved in cholesterol biosynthesis, including HMG*CR* and SREBP2 itself (20). In line with the abnormal localization of SREBP2 in HD cortex, I also found that the transcription of SREBP2 target genes, specifically *HMGCR*, and *SREBP2,* was significantly down-regulated HD mouse brain cortex when compared to controls.

Taken together, these findings suggest that altered cholesterol biosynthesis in HD is likely due to the interference of mHtt with the normal nuclear translocation of SREBP2. In support of this hypothesis, immunofluorescence analysis showed that in HD cells overexpressing tagged mSREBP2 (mSREBP2-EGFP), at least in part the chimeric protein was localized in the cytoplasm of HD cell lines. Similar results were observed in primary neurons from YAC128 mice and interestingly also in fibroblasts from HD patients.

A major pathological feature of HD is the formation of insoluble aggregates of mHtt which are able to sequester transcription factors, thus decreasing their availability in the nucleus and altering the expression of target genes (22, 23).

In our study we demonstrated that the retention of mSREBP2 in the cytoplasm of HD was not due to its sequestration into aggregates of mHtt, but rather to physical interaction with the mutant protein in the cytoplasm of HD cells. This was shown by co-immunoprecipitation studies where mHtt co-immunoprecipitated in complex with mSREBP2. In experiments where Htt was overexpressed I could also observe some wild-type Htt co-immunoprecipitating with mSREBP2 from cytoplasmic fractions of transfected cells, but to a much smaller extent than with mHtt. Much less interaction with wild-type Htt, if any, was found in models that expressed physiological levels of Htt (knock-in cells as well as wild-type brain),

suggesting that the observed interaction between wild-type Htt and mSREBP2 in the cytoplasm of normal cells might be an artifact of protein overexpression. Alternatively, wild-type Htt might interact with mSREBP2 with much weaker affinity or more transiently than mHtt. Interestingly, when I immunoprecipitated mSREBP2 from nuclear fractions, both wild-type and mHtt were found in complex with the transcription factor in similar amounts, suggesting that in the nucleus Htt might be part of a transcriptional complex with mSREBP.

The majority of cytosolic proteins enter the nucleus through the classical nuclear transport by binding a heterodimer of importin-alpha and importin-beta. Conversely, as previously described, mSREBP2 does not require the presence of importin-alpha and enters the nucleus through a non-classical nuclear transport, by direct binding to importin-! (19, 24).

This alternative mode of nuclear entry is quite unique for SREBP and a few other proteins (25, 26).

Classic nuclear transport was not affected in HD cells, as shown by correct nuclear targeting of a chimeric NLS-containing protein (GST-NLS-EGFP). Therefore, mHtt specifically affected the alternative pathway of nuclear entry and/or mSREBP2 interaction with importin-! .

Importing beta has been shown to bind SREBP proteins through a protein region known as HEAT domain. The name of this domain involved in protein-protein interactions derives from the proteins where the domain was first identified: Huntingtin elongation factor 3 (EF3), protein phosphatase 2A (PP2A), and the yeast kinase TOR1 (19). Because Htt contains several HEAT domains, we hypothesized that it competes with importin-! for the binding to mSREBP2 in HD cells, thus disrupting mSREBP2 nuclear import.

However, contrary to our expectations, we found that not only mHtt does not interfere with the binding of mSREBP2 to importin-! , but it actually stabilizes this interaction. This is suggested by the fact that more importin-! was found in complex with mSREBP2 in HD than in normal cells.

Since mHtt, mSREBP2 and importin-! were always co-immunoprecipitated together, we asked the question of whether mHtt interacted with SREBP2 directly or through binding to importin-! . To answer this question we exposed the immunoprecipitated complex to saturating concentrations of RanGTP. In the nucleus of normal cells RanGTP binds importin-! and triggers a conformational change in this protein that results in the release of importin-! from its cargo.

When I added purified RanGTP to the immunoprecipitated complex, importin-! was dissociated from mSREBP2, as expected, and released into the supernatant, while both SREBP2 and mHtt remained attached to the beads, demonstrating that mHtt binds to mSREBP2 independently of importin-! . Future studies will examine whether the impairment of SREBP2 transport to the nucleus in HD cells is specific for SREBPs or generalized to other cargo proteins, such as SMADs, that are transported to the nucleus by direct binding to importin-! (26).

The studies presented in this thesis have uncovered a novel toxic effect of mHtt and shed light on the mechanism underlying defective cholesterol biosynthesis in HD. All together my findings indicate that cholesterol dysregulation in HD stems from an aberrant interaction between mHtt and SREBP2. Whether this is a direct interaction, or rather mediated by other proteins remains to be determined.

2.5. **FIGURES**

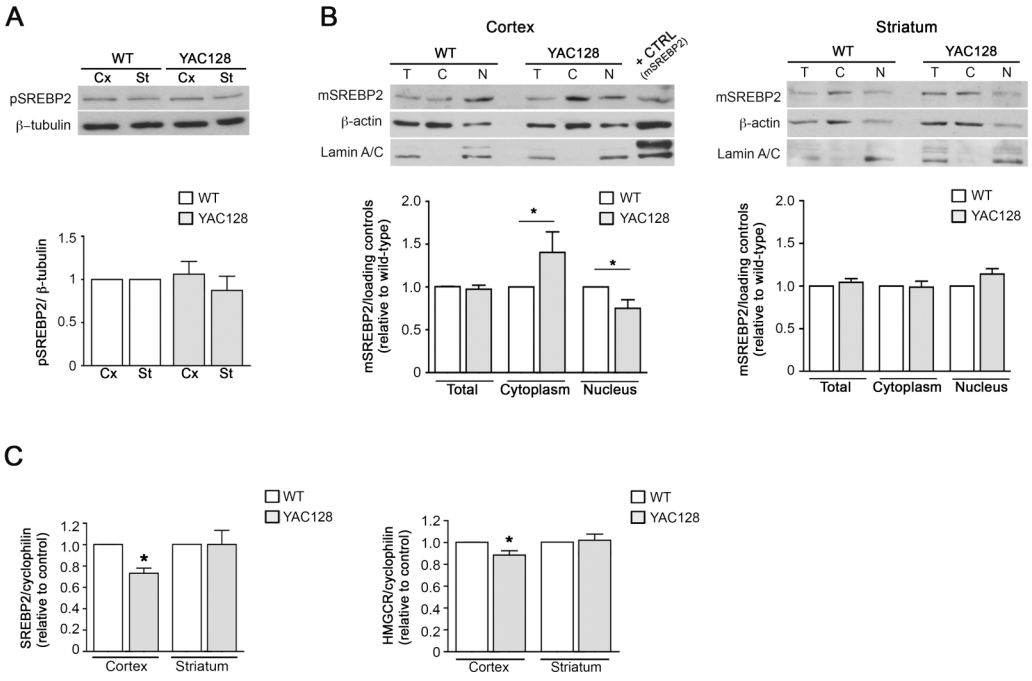

Figure 2.1 Decreased mature SREBP2 in the nuclear fraction of YAC128 cerebral cortex correlates with decreased SREBP2-dependent gene transcription. A) Representative immunoblot showing that levels of the precursor form of SREBP2 (pSREBP2) are similar in total lysates of 6 month-old WT and YAC128 cerebral cortex (Cx) and striatum (St). The graph shows the mean densitometric values ± SD calculated over 4 mice per genotype. **B)** Total (T), cytoplasmic (C) and nuclear (N) fractions were prepared from cerebral cortex and striatum of WT and YAC128 mice and probed with anti-SREBP2 antibody to detect the cleaved mature form of SREBP2 (mSREBP2). A positive control (+ CTRL) for mSREBP2 expression was generated by transient transfection of STHdh7/7 cells with mSREBP2 cDNA. Representative immunoblots are shown. Graphs show the densitometric analysis of 3 independent experiments. ! -actin was used as loading control for total and cytoplasmic fractions, lamin A/C was used as a loading control for nuclear fractions. **C)** Expression of SREBP2 and HMGCoA reductase (HMGCR), were decreased in the cortex, but not in the striatum of 6 month-old YAC128 mice, as measured by real-time PCR. Data were normalized over cyclophilin expression and expressed as ratio over WT. *p<0.05.

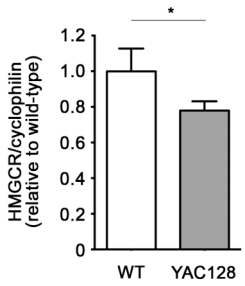

Figure 2.2 Decreased expression of HMG-CoA reductase in the striatum of 9 month-old YAC128 mice. Expression of HMGCoA reductase (HMGCR) was measured by real-time PCR. Data were normalized over cyclophilin expression and expressed as ratio over WT. *p<0.05.

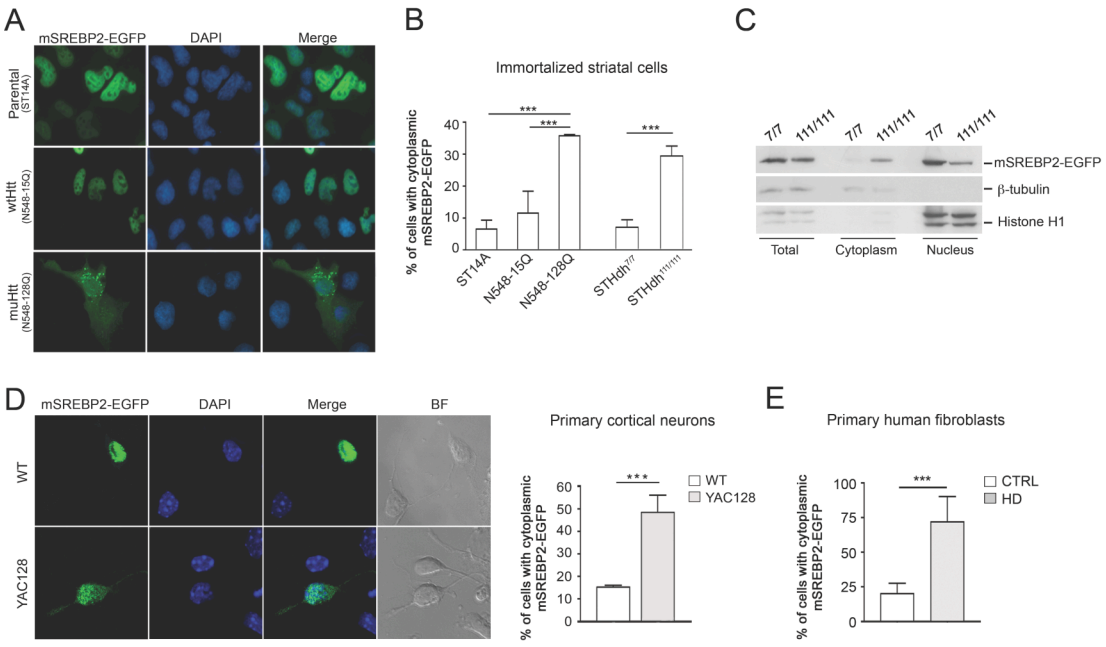

Figure 2.3. mSREBP2-EGFP is mislocalized in the cytoplasm of HD cells. Confocal microscopy images showing the intracellular localization of transiently transfected mSREBP2-EGFP in parental cells (ST14A) and in cells expressing an N-terminal fragment of wild-type (N548-15Q) or mutant (N548-128Q) Htt. Cell nuclei were counterstained with DAPI. **B)** Percentage (mean ± SD) of cells with cytoplasmic localization of mSREBP2-pEGFP after transient transfection of the indicated cell lines with the chimeric protein. A minimum of 80 mSREBP2-EGFP expressing-cells per cell line was counted in each of three independent experiments. $^{***}p<0.001$. **C)** Immunoblot showing the subcellular distribution of mSREBP2-EGFP in STHdh$^{7/7}$ (7/7) and STHdh$^{111/111}$ (111/111) knock-in cells following transient cell transfection and subcellular fractionation. Tubulin and histone H1 were used as loading controls for total/cytoplasmic and nuclear fractions, respectively. Data were normalized over wild-type cells. **D)** Localization of mSREBP2-EGFP in primary WT and YAC128 cortical neurons (10 DIV). Confocal microscopy images were taken 24 hours after nucleofection of neurons with mSREBP2-EGFP. Nuclei were counterstained with DAPI. The percentage of neurons with cytoplasmic localization of mSREBP2-EGFP is shown in the bar graph. Data are the mean ± SD of three independent experiments. A minimum of 100 cells per genotype was counted. BF, bright field. **E)** Extranuclear localization of mSREBP2-EGFP in transiently transfected human fibroblasts isolated from normal subjects (CTRL) or HD patients. $^{***}p<0.001$

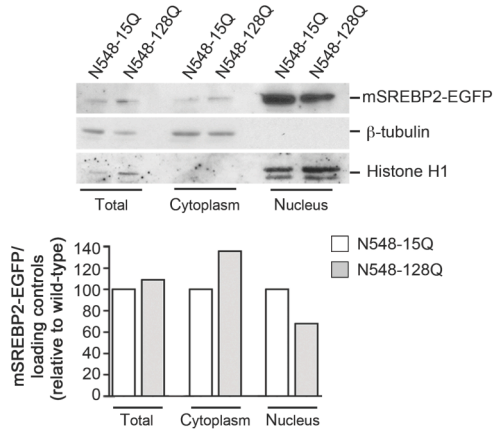

Figure 2.4. Immunoblot and densitometric analysis showing the subcellular distribution of transiently transfected mSREBP2-EGFP in cells expressing an N-terminal fragment of wild-type (N548-15Q) or mutant (N548-128Q) Htt. Tubulin and histone H1 were used as loading controls for total/cytoplasmic and nuclear fractions, respectively. Data were normalized over wild-type cells.

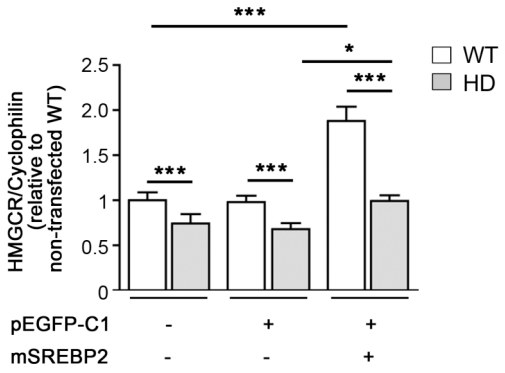

Figure 2.5. HMGCoA reductase expression after cell transfection with mSREBP2 is increased to a greater extent in normal than in HD primary fibroblasts. Primary fibroblasts from normal or HD patients were co-transfected with pEGFP-C1 and mSREBP2 (1:10 ratio). Transfected cells were sorted by fluorescence-activated cell sorter and used for mRNA extraction and real-time PCR. Average expression of HMGCoA reductase (HMGCR), normalized over cyclophilin and relative to non transfected cells is shown. *p<0.05; ***p<0.001.

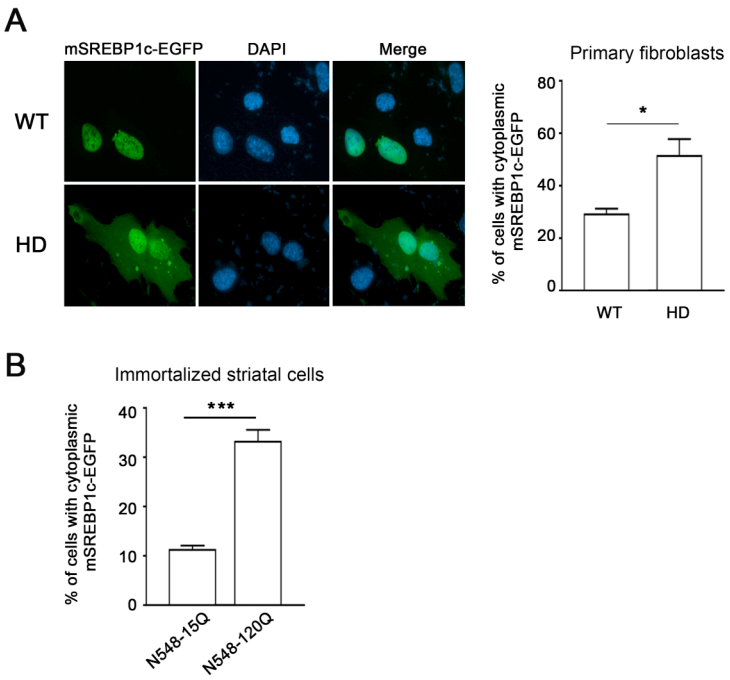

Figure 2.6. mSREBP1c-EGFP is mislocalized in the cytoplasm of HD cells. A) Confocal microscopy images showing the intracellular localization of transfected mSREBP1c-EGFP in normal and HD human primary fibroblasts. The graph shows the percentage of cells with cytoplasmic localization of the chimeric protein. Data are means ± SD of three independent experiments. B) Immortalized striatal cells expressing a N-terminal fragment of wild-type (N548-Q15) or mutant (N548-Q128) Htt were transfected with mSREBP1c-EGFP and the number of cells with cytoplasmic localization of the chimera was counted. Data are the mean ± SD of three independent experiments. $^{*}p<0.05$; $^{***}p<0.001$.

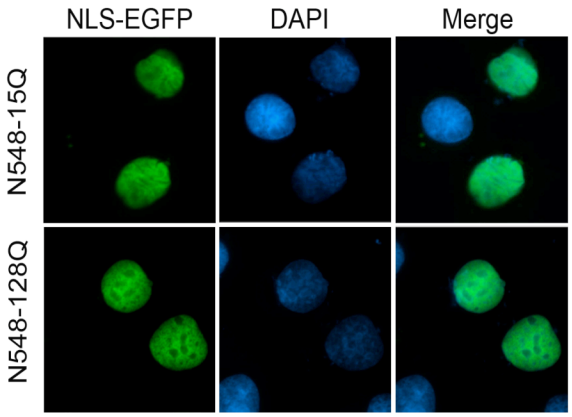

Figure 2.7. The classic nuclear import is not affected in HD cells. Representative confocal microscopy images of immortalized striatal cells expressing an N-terminal fragment of Htt (N548) with 15Q (WT) or 128Q (HD), and transiently transfected with EGFP fused to the classic nuclear localization sequence (NLS-EGFP). The chimeric protein is detected only in the nucleus, both in WT and HD cells.

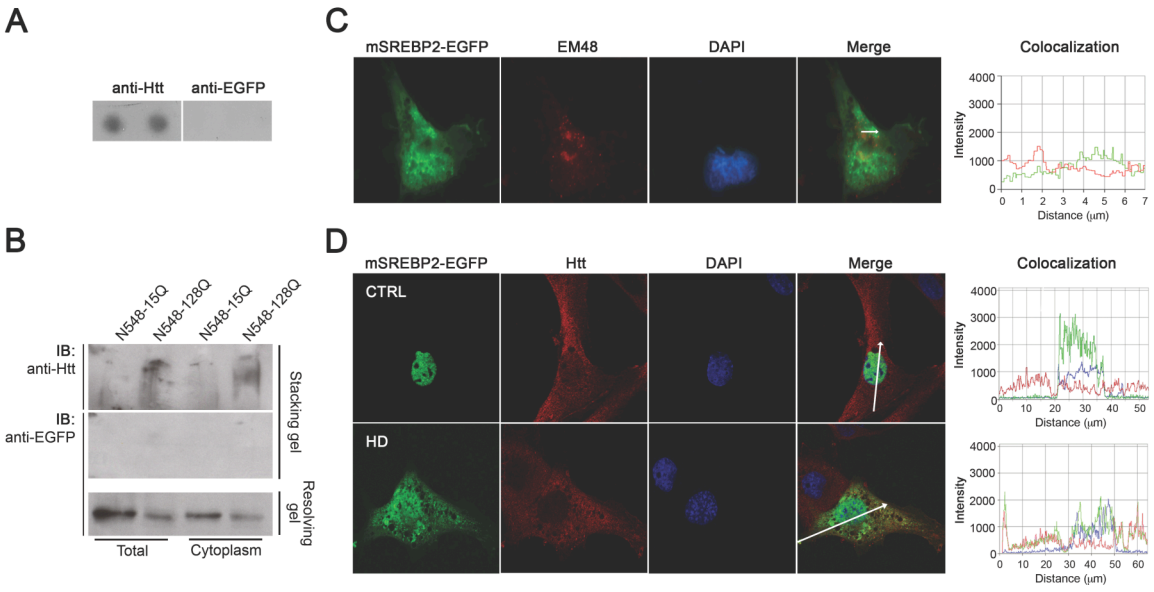

Figure 2.8. mSREBP2-EGFP co-localizes with soluble mHtt, but is not sequestered into insoluble huntingtin aggregates. A) Filter trap retention assay performed on total cell lysate from N548-128 cells, 24 hours after transfection with mSREBP2-EGFP. MHtt aggregates trapped on cellulose acetate membrane filter were detected with anti-Htt antibodies (mAb2166). No mSREBP2-EGFP was detected in the insoluble material using anti-GFP antibodies. **B)** Total cell lysate and cytoplasmic fraction isolated from N548-15Q and N548-128Q cells after transfection with mSREBP2-EGFP were separated on SDS-PAGE. Insoluble aggregates of mHtt were detected in the stacking gel by immonoblotting with anti-Htt antibodies (mAb2166). mSREBP2-EGFP was detected in the resolving gel, but not in the stacking gel. **C)** Representative confocal images and fluorescence intensity profiles of N548-128 cells transfected with mSREBP2-EGFP and immunostained with EM48 antibodies to detect mHtt inclusions. The line-scan graph shows lack of co-localization between the signal generated by EM48 (red line) and mSREBP2-EGFP (green line). **D)** Representative confocal microscopy images and fluorescence intensity profiles of primary human fibroblast transiently transfected with mSREBP2-EGFP and immunostained with anti-Htt antibodies (PW095). The line-scan graphs show the immunofluorescence intensity of Htt (red line) and mSREBP2-EGFP (green line) signals along the white arrow, and colocalization of mSREBP2-EGFP with Htt in the cytoplasm of HD cells.

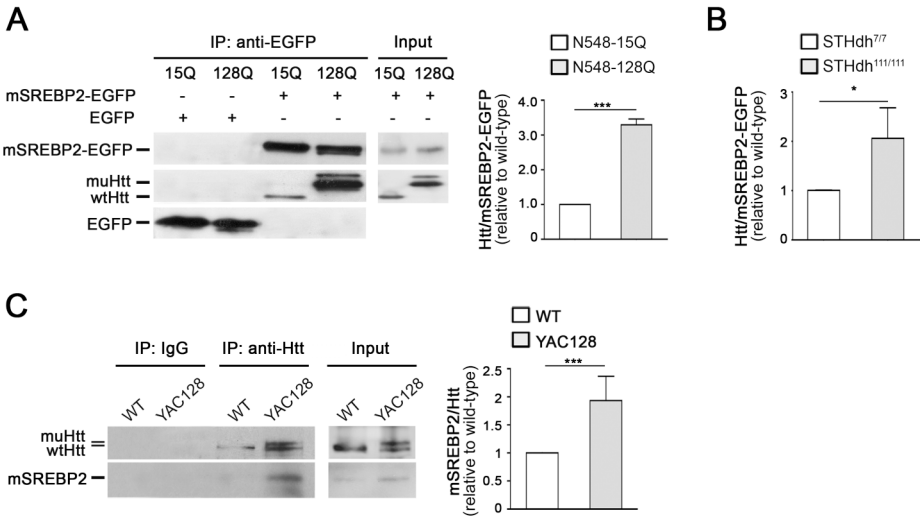

Figure 2.9. mSREBP2 co-immunoprecipitates with mHtt from cytoplasmic fractions of HD cells and brains. A) mSREBP2-EGFP was transiently transfected in striatal cells expressing wild-type (15Q) or mutant (128Q) Htt N-terminal fragments (N548) and immunoprecipitated from cytoplasmic cell fractions using anti-EGFP antibodies. MHtt fragments were co-immunoprecipitated to a greater extent than wild-type fragments. Nor wild-type neither mHtt interacted with the control protein, EGFP. A representative immunoprecipitation is displayed, while the graph shows the mean densitometric ratios ± SD of four independent experiments. B) mSREBP-EGFP co-immunoprecipitate with full-length mHtt from the cytoplasmic fraction of STHdh$^{111/111}$. The graph shows the mean ratio Htt/mSREBP2-EGFP ± SD of three independent experiments. See also Figure 5A for a representative immunoblot. **C)** Htt was immunoprecipitated from cytoplasmic fractions prepared from WT and YAC128 mouse cerebral cortex. Endogenous mSREBP2 co-immunoprecipitated with Htt from YAC128 tissue, to a much greater extent than from WT tissue. The graph shows the mean mSREBP2/Htt ratio ± SD measured after protein immunoprecipitation from three mouse brains per genotype. *, p<0.05; ***, p<0.001

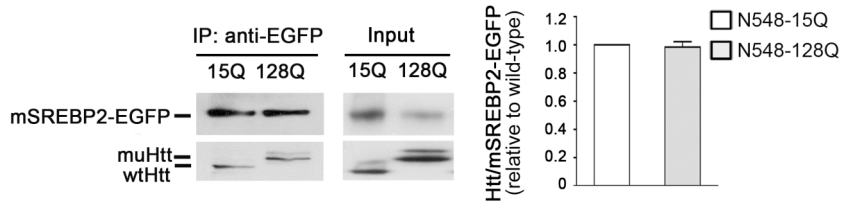

Figure 2.10. Both wild-type and mHtt co-immunoprecipitate with mSREBP2-EGFP from nuclear fractions of HD cells. mSREBP2-EGFP was transiently transfected in striatal cells expressing wild-type (15Q) or mutant (128Q) Htt N-terminal fragments (N548 aa.). mSREBP2-EGFP was immunoprecipitated from nuclear fractions using anti-GFP antibodies. The graph shows the densitometric analysis of 3 experiments. Data are expressed as mean ratios relative to control ± SD.

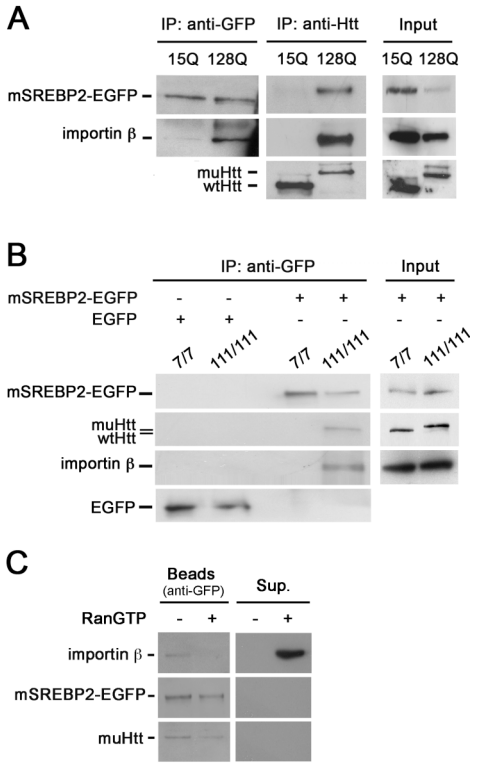

Figure 2.11. MHtt is in a complex with and stabilizes the interaction between mSREBP2 and importin-β . A) Immunoblotting showing that more importin-! co-immunoprecipitates with mSREBP2-EGFP from cells expressing mHtt (N548-128Q) than from cells expressing wilt-type Htt (N548-15Q). Importin-! is also co-immunoprecipitated by anti-Htt antibodies in complex with mHtt fragments (N548-128Q) and mSREBP2-EGFP. **B)** Immunoblotting showing that importin-! co-immunoprecipitates with mSREBP2-EGFP and full-length mHtt from STHdh$^{111/111}$ (111/111) cytoplasmic fractions, in spite of similar levels of importin-! being expressed in the two cell lines. 7/7, STHdh$^{7/7}$. **C)** RanGTP (5 $M) was added to the mSREBP2-EGFP/mHtt/importin-! complex immunoprecipitated using anti-GFP antibody, in order to trigger the release of importin-! from its cargo. In the presence of RanGTP importin-! was released in the supernatant, but mHtt remained in the pellet (beads), indicating that mHtt does not directly interact with importin-! in these experimental conditions.

2.6. REFERENCES

1. Valenza M, Rigamonti D, Goffredo D, Zuccato C, Fenu S, Jamot L, Strand A, Tarditi A, Woodman B, Racchi M, Mariotti C, Di Donato S, Corsini A, Bates G, Pruss R, Olson JM, Sipione S, Tartari M, Cattaneo E. (2005) Dysfunction of the cholesterol biosynthetic pathway in Huntington's disease. J Neurosci. Oct 26;25(43):9932-9.
2. Valenza M, Carroll JB, Leoni V, Bertram LN, Björkhem I, Singaraja RR, Di Donato S, Lutjohann D, Hayden MR, Cattaneo E. (2007) Cholesterol biosynthesis pathway is disturbed in YAC128 mice and is modulated by huntingtin mutation. Hum Mol Genet. Sep 15;16(18):2187-98.
3. Valenza M, Leoni V, Tarditi A, Mariotti C, Björkhem I, Di Donato S, Cattaneo E. (2007) Progressive dysfunction of the cholesterol biosynthesis pathway in the R6/2 mouse model of Huntington's disease. Neurobiol Dis. Oct;28(1):133-42.
4. Valenza M, Leoni V, Karasinska JM, Petricca L, Fan J, Carroll J, Pouladi MA, Fossale E, Nguyen HP, Riess O, MacDonald M, Wellington C, DiDonato S, Hayden M, Cattaneo E. (2010) Cholesterol defect is marked across multiple rodent models of Huntington's disease and is manifest in astrocytes. J Neurosci.Aug 11;30(32):10844-50
5. Dietschy JM, Turley SD. (2004) Thematic review series: brain Lipids. Cholesterol metabolism in the central nervous system during early development and in the mature animal. J Lipid Res. Aug;45(8):1375-97.
6. Brown MS, Goldstein JL. (1997) The SREBP pathway: regulation of cholesterol metabolism by proteolysis of a membrane-bound transcription factor. Cell. May 2;89(3):331-40.
7. Jeon TI, Osborne TF. (2012) SREBPs: metabolic integrators in physiology and metabolism. Trends Endocrinol Metab. Feb;23(2):65-72.
8. Hua X, Wu J, Goldstein JL, Brown MS, Hobbs HH. (1995) Structure of the human gene encoding sterol regulatory element binding protein-1 (SREBF1) and localization of SREBF1 and SREBF2 to chromosomes 17p11.2 and 22q13. Genomics. Feb 10;25(3):667-73.
9. Brown MS, Goldstein JL. (1997) The SREBP pathway: regulation of cholesterol metabolism by proteolysis of a membrane-bound transcription factor. Cell. May 2;89(3):331-40.
10. Yang T, Espenshade PJ, Wright ME, Yabe D, Gong Y, Aebersold R, Goldstein JL, Brown MS. (2002) Crucial step in cholesterol homeostasis: sterols promote

binding of SCAP to INSIG-1, a membrane protein that facilitates retention of SREBPs in ER. Cell. Aug 23;110(4):489-500.

11. Yabe D, Brown MS, Goldstein JL. (2002) Insig-2, a second endoplasmic reticulum protein that binds SCAP and blocks export of sterol regulatory element-binding proteins. Proc Natl Acad Sci U S A. Oct 1;99(20):12753-8.
12. Rigamonti D, Bauer JH, De-Fraja C, Conti L, Sipione S, Sciorati C, Clementi E, Hackam A, Hayden MR, Li Y, Cooper JK, Ross CA, Govoni S, Vincenz C, Cattaneo E. (2000) Wild-type huntingtin protects from apoptosis upstream of caspase-3. J Neurosci. May 15;20(10):3705
13. Sipione S, Rigamonti D, Valenza M, Zuccato C, Conti L, Pritchard J, Kooperberg C, Olson JM, Cattaneo E. (2002) Early transcriptional profiles in huntingtin-inducible striatal cells by microarray analyses. Hum Mol Genet. Aug 15;11(17):1953-65.
14. Zheng Z, Diamond MI. (2012) Huntington disease and the huntingtin protein. Prog Mol Biol Transl Sci. 107:189-214.
15. Lee SJ, Sekimoto T, Yamashita E, Nagoshi E, Nakagawa A, Imamoto N, Yoshimura M, Sakai H, Chong KT, Tsukihara T, Yoneda Y. (2003) The structure of importin-beta bound to SREBP-2: nuclear import of a transcription factor. Science. Nov 28;302(5650):1571-5.
16. Battaile KP, Steiner RD. (2000) Smith-Lemli-Opitz syndrome: the first malformation syndrome associated with defective cholesterol synthesis. Mol Genet Metab.Sep-Oct;71(1-2):154-62.
17. Mahley RW, Huang Y, Rall SC Jr. (1999) Pathogenesis of type III hyperlipoproteinemia (dysbetalipoproteinemia). Questions, quandaries, and paradoxes. J Lipid Res. Nov;40(11):1933-49.
18. Leoni V, Mariotti C, Tabrizi SJ, Valenza M, Wild EJ, Henley SM, Hobbs NZ, Mandelli ML, Grisoli M, Björkhem I, Cattaneo E, Di Donato S. (2008) Plasma 24S-hydroxycholesterol and caudate MRI in pre-manifest and early Huntington's disease. Brain. Nov;131(Pt 11):2851-9.

Lee SJ, Sekimoto T, Yamashita E, Nagoshi E, Nakagawa A, Imamoto N, Yoshimura M, Sakai H, Chong KT, Tsukihara T, Yoneda Y. (2003) The structure of importin-beta bound to SREBP-2: nuclear import of a transcription factor. Science. Nov 28;302(5650):1571-5.

Amemiya-Kudo M, Shimano H, Hasty AH, Yahagi N, Yoshikawa T, Matsuzaka T, Okazaki H, Tamura Y, Iizuka Y, Ohashi K, Osuga J, Harada K, Gotoda T, Sato R, Kimura S, Ishibashi S, Yamada N. (2002) Transcriptional activities of nuclear

SREBP-1a, -1c, and -2 to different target promoters of lipogenic and cholesterogenic genes. J Lipid Res. Aug;43(8):1220-35.

Bano D, Zanetti F, Mende Y, Nicotera P. (2011) Neurodegenerative processes in Huntington's disease. Cell Death Dis. Nov 10;2:e228.

Cha JH. (2000) Transcriptional dysregulation in Huntington's disease. Trends Neurosci. Sep;23(9):387-92.

Li SH, Li XJ. (2004) Huntingtin and its role in neuronal degeneration. Neuroscientist. Oct;10(5):467-75.

Nagoshi E, Imamoto N, Sato R, Yoneda Y. (1999) Nuclear import of sterol regulatory element-binding protein-2, a basic helix-loop-helix-leucine zipper (bHLH-Zip)-containing transcription factor, occurs through the direct interaction of importin-! with HLH-Zip. Mol Biol Cell. Jul;10(7):2221-33.

Forwood JK, Lam MH, Jans DA. (2001) Nuclear import of Creb and AP-1 transcription factors requires importin-beta 1 and Ran but is independent of importin-alpha. Biochemistry. May 1;40(17):5208-17.

Chen X, Xu L. Mechanism and regulation of nucleocytoplasmic trafficking of smad. (2011) Cell Biosci. Dec 28;1

3. CHAPTER 2

This chapter has been published as:

Di Pardo A, Maglione V, Alpaugh M, Horkey M, Atwal RS, Sassone J, Ciammola A, Steffan JS, Fouad K, Truant R, Sipione S. (2012). Ganglioside GM1 induces phosphorylation of mutant huntingtin and restores normal motor behavior in Huntington disease mice. *Proc Natl Acad Sci U S A:*109(9):3528-33. doi: 10.1073/pnas.1114502109.

THERAPEUTIC POTENTIAL OF GANGLIOSIDE GM1 FOR THE TREATMENT OF HD

3.1. INTRODUCTION

Huntington disease (HD) is an inherited neurodegenerative monogenic disorder caused by the expansion of a polyglutamine stretch beyond 36 residues in the amino-terminal domain of huntingtin (Htt), a protein expressed in most tissues and cells. The mutation causes huntingtin to acquire toxic conformation/s and to affect neuronal function and viability. Medium-sized spiny neurons (MSNs) in the corpus striatum are most affected, but neurodegeneration also occurs in the cerebral cortex and, to a minor extent, in other brain areas, resulting in motor and psychiatric symptoms, as well as cognitive decline. The cellular and molecular mechanisms underlying HD pathogenesis are complex. Both loss and gain of function of mutant huntingtin contribute to cause a wide array of neuronal dysfunctions affecting cell signaling, gene transcription, axonal transport, cell and mitochondrial metabolism as well as neurotransmission (1).

In recent years, a breakthrough in HD research has been the discovery that posttranslational modifications of mHtt are crucial modulators of mHtt toxicity (2–4). Phosphorylation at various serine residues prevents cleavage of mutant huntingtin into more toxic fragments, decreases neural cell death in vitro (5–10), and/or restores Htt functions that are compromised by the mutation (8, 11). The most dramatic effects have been described for huntingtin phosphorylation at serine 13 and serine 16. These two amino acid residues are part of the highly conserved amino-terminal **"**N17**"** domain of huntingtin, a domain that regulates huntingtin intracellular localization and association to cellular membranes (12, 13), as well as kinetics of mutant huntingtin aggregation (14, 15). Phosphomimetic mutations of serine 13 and serine 16 by aspartic or glutamic acid substitution (S13D and S16D or S13E and S16E) decrease the toxicity of mutant huntingtin fragments in vitro (10, 16). In line with these studies, expression of a phosphomimetic (S13D and S16D) mutant

form of expanded full-length huntingtin in a BACHD transgenic mouse model was shown to result in a normal phenotype, with no detectable signs of HD pathology by 12 months (17).

These findings suggest that pharmacological interventions that modulate cell signaling and mutant huntingtin phosphorylation might slow down or even stop disease progression. Recently, we and other groups reported that levels of GM1, a ganglioside involved in cell signaling (18), are decreased in HD models (19–21), in fibroblasts isolated from HD patients (19), and in postmortem human HD brain samples (20, 21). Gangliosides are sialic acid-containing glycosphingolipids highly abundant in the brain, where they exert a plethora of important cell regulatory functions (18). They are major components of membrane microdomains known as "lipid rafts" (22) and are important players in cell signaling (23) and cell–cell interaction (24). By influencing membrane properties and/or by direct interaction with membrane proteins, gangliosides modulate the activity of many tyrosine kinase (25–28) and neurotransmitter receptors (29), ion channels (30, 31), and downstream cell signaling pathways. In addition, gangliosides regulate axon–myelin communication and the maintenance of myelinated axons in the adult central and peripheral nervous systems (32–34). Consistent with the pivotal role of gangliosides in the nervous system and in cell signaling, defects in their biosynthetic pathway lead to a severe infantile neurodegenerative disorder characterized by progressive brain atrophy, chorea, and epilepsy (35), symptoms that are also common to the juvenile form of HD (36). We hypothesized that in HD, decreased GM1 levels contribute to neuronal dysfunction and disease pathogenesis. Supporting this hypothesis, we demonstrated that restoring normal GM1 levels in an HD neural cell line stimulates the activation of prosurvival cell signaling pathways and provides protection from apoptosis. As a corollary, inhibiting GM1 synthesis in wild-type striatal cells recapitulates the increased susceptibility to apoptosis that is observed in HD neuronal cells (19). In this study, we have explored the therapeutic potential of restoring GM1 levels in a transgenic HD mouse model.

We demonstrate that GM1 infusion abrogates the motor deficit of yeast artificial chromosome (YAC)128 mice, an effect that is accompanied by increased expression and activation of striatal dopamine and adenosine 3′,5′-monophosphate–regulated phosphoprotein (32 kDa) (DARPP-32), as well as phosphorylation of huntingtin at serine 13 and serine 16, in vivo.

3.2. MATERIAL AND METHODS

3.2.1. Animal Models

YAC128 mice were purchased from The Jackson Laboratory and maintained in our animal facility at the University of Alberta. All procedures on animals were approved by the University of Alberta's Animal Care and Use Committee and were in accordance with the guidelines of the Canadian Council on Animal Care. All in vivo experiments were performed in 5- to 6-mo-old male YAC128 mice and WT littermates that showed no sign of distress and weighed no less than 26 g and no more than 34 g.

3.2.2. Cell Models

Conditionally immortalized mouse striatal knock-in cells expressing endogenous levels of WT (STHdh7/7) or mutant huntingtin (STHdh111/111) were a gift from M. E. MacDonald (Massachusetts General Hospital, Boston) and were maintained in culture as previously described (1). Human skin fibroblasts isolated from HD patients (lines GM03621 and GM04208, each expressing one mutant HD allele with 61 and 45 CAG repeats, respectively) were purchased from Coriell Cell Repositories and grown as previously described (2). Cultures of primary striatal neurons were prepared from newborn mice (P0) as previously described (2).

3.2.3. Chronic GM1 Administration in Vivo

A microcannula was stereotaxically inserted into the right ventricle (1.25 mm right lateral and 0.6 mm posterior to bregma, 3mm deep) of anesthetized mice, and connected to an osmotic pump (Alzet; model 2004) that was implanted s.c. on the back of the mouse. The pump infused a solution of 3.6 mM GM1 in artificial CSF into the brain ventricle at a constant rate (0.25 L/h) for 28 d. On the basis of volume and rate of synthesis/ renewal of the mouse CSF (57), these conditions result in a concentration of 50 M GM1 in the

mouse CSF at equilibrium. Experiments were performed with both natural GM1 (highly purified, ≥98%, from bovine brain; Alexis) and synthetic GM1 provided by Seneb BioSciences Inc., with virtually identical results. Animals were monitored on a daily basis for signs of treatment-related toxicity, such as poor grooming, lethargy, loss of body weight, and abnormal behavior.

3.2.4. Huntingtin Immunoprecipitation and Immunoblotting

Conditionally immortalized mouse striatal knock-in cells expressing endogenous levels of WT (STHdh7/7) or mutant huntingtin (STHdh111/111), were incubated with 50 M GM1 for 10 min or 5 h and then lysed in 20mMTris, pH 8.0, 150mM NaCl, 1% Triton X-100, 0.5% Na-deoxycholate, 0.1% SDS, 1 mM EDTA, 1 mM EGTA, containing protease inhibitor mixture (1:100; Sigma-Aldrich), 50 M proteosomal inhibitor MG132 (Sigma-Aldrich), and phosphatase inhibitors (20 mM NaF, 2 mM Na3VO4). Cells were homogenized through a 26-gauge syringe needle and sonicated three times, 10 s each, followed by incubation on ice for 30 min. Lysates were centrifuged at 10,000 Å~ g for 10min to remove debris. Immunoprecipitation was performed on 0.8 mg of total lysate using polyclonal anti-huntingtin (N17) or anti-phospho huntingtin (pN17) (16) complexed to protein G sepharose (Zymed, Invitrogen). The immunoprecipitated protein was resolved on 6% SDS/PAGE and transferred overnight on PVDF membrane (Millipore) in 25 mM Tris, 192 mM glycine containing 0.05% SDS and 16% methanol. These transfer conditions allow for optimal transfer of high molecular-weight forms of huntingtin. Huntingtin detection was performed by immunoblotting with polyclonal anti-huntingtin (PW0595 and N17; 1:10,000), polyclonal anti-pN17 antibody (1:10,000 (16), monoclonal anti-huntingtin (mAb2166, 1:5,000; Chemicon), polyclonal antipSer13 (1:1,000), and anti-pSer16 (1:500 (10). HRP-conjugated secondary antibodies were used at 1:10,000 dilution (Bio-Rad Laboratories). Protein bands were detected by ECL Plus and quantitated with Quantity One software (Bio-Rad Laboratories).

3.2.5. Motor Behavior Tests

All behavior tests were carried out during the light phase of the light/dark cycle. Six mice per experimental group were used in each test. In order to establish a baseline and the effect of GM1 on motor function, mice were tested before and after implantation of the Alzet pump at the indicated time points. Before training and testing, mice underwent a period of habituation to the testing room and equipment. All mice received training for 2 consecutive days on each instrument and task before performing motor behavior measurements. Mice were tested at fixed speed (20 rpm) on a rotarod apparatus (Ugo Basile) for 1 min. Each mouse was tested in three consecutive trials of 1 min each, with 1 min rest between trials. The time spent on the rotarod in each of the three trials was averaged to give the overall time for each mouse. A similar training protocol was used to test the mice on an accelerating rotarod (from 4 to 40 rpm in 1 min). In the narrow beam test, mice were placed at the extremity of a 100-cm-long wooden narrow beam (0.75 cm wide, suspended 30 cm above the floor) and allowed to traverse the beam from one extremity to the other three times. During the test, animal performance was recorded with a videocamera. The number of footfalls (errors) was counted in each crossing, the balance control, the number of slips and body coordination were evaluated during the walking and were analyzed frame by frame and using a footfall scoring system. In the horizontal ladder task, mice were recorded with a videocamera as they spontaneously walked along a horizontal ladder with variable and irregular spacing between rungs. In each test session, the mouse performance was evaluated using an established footfall scoring system (3), which allows for qualitative and quantitative evaluation of forelimb and hindlimb placement on the ladder rungs. All motor tests were conducted by the same experimenter who was blinded to mouse genotype and experimental group throughout the entire course of the analysis.

3.2.6. Immunocytochemistry

Knock-in cells were grown on glass coverslips coated with 50 g/mL poly-L-lysine and treated with GM1 (Alexis; 50 M) for 5 h. Cells were then washed in Dulbecco's PBS (DPBS), fixed in 4% paraformaldehyde for 10 min at room temperature (RT) and permeabilized with 0.5% Triton X-100 in PBS for 5 min. After blocking with 4% donkey serum in PBS for 1 h, cells were in- cubated with polyclonal rabbit pN17 antibody (1:1,000) for 1 h at RT. Antirabbit Alexa 488- and Alexa 555-conjugated secondary antibodies (Molecular Probes, Invitrogen) were used at 1:500 dilution for 1 h at RT. Cell nuclei were stained with 4",6 dia-midino-2-phenildindole (DAPI) (Vector Laboratories) for 10 min at RT. Coverslips were mounted using Prolong Gold antifade reagent (Molecular Probes, Invitrogen).

Confocal analysis was performed using an LSM510 laser scanning confocal microscope mounted on a Zeiss Axiovert 100M microscope. Images of untreated and GM1-treated cells were acquired using the same confocal settings. The mean fluorescence intensity (MFI) per pixel in each cell was calculated with ImageJ software (National Institutes of Health) after manual selection of cell area.

3.2.7. Dot-Blotting for GM1

Fifty picograms of proteins from total lysates prepared from cortical and striatal tissue were spotted on ni- trocellulose membrane using a dot-blot apparatus (Bio-Rad). Membranes were then blocked in 5% milk in TBS-T and in- cubated with HRP-conjugated cholera toxin B (5 g/mL) for 30 min at room temperature. Densitometric analysis was performed after ECL chemiluminescence detection using Quantity One software (Bio-Rad).

3.2.8. Brain Lysate Preparation and Immunoblotting

Mice were euthanized by cervical dislocation, brain regions including cortex and striatum were dissected out, snap frozen in liquid N2, and pulverized in a mortar with a pestle. Pulverized tissue was homogenized in lysis buffer containing 10 mM Tris, pH 7.4, 1% Nonidet P-40, 1 mM EGTA, 1 mM EDTA, 50 M proteosomal inhibitor MG132 (Sigma-Aldrich), 20 mM NaF, 2 mM Na3V04, and 1:100 protease inhibitor mixture (Sigma-Aldrich), sonicated with 2 %10 s pulses and then centrifuged for 10 min at 10,000 %g. Fifty micrograms of supernatant proteins were re- solved on 6% SDS/PAGE and detected by immunoblotting with polyclonal anti-pN17 (1:8,000 dilution in Li-Cor blocking buffer) and monoclonal ant-talin (clone 8d4; Sigma; 1:1,000) and anti-huntingtin (mAb2166; 1:5,000; Chemicon) antibodies. For analysis of DARPP-32 expression, 30 g of total lysate from striatum were immunoblotted with anti–DARPP-32 (BD Transduction Laboratories; 1:1,000 dilution) or anti–pDARPP-32(Thr34) (Cell Signaling; 1:1,000 dilution) antibodies. IR dye 800/680CW-conjugated secondary antibodies were used at 1:10,000 dilution. Relative protein quantitation was performed using an Odyssey Infrared Imaging system (Li-Cor).

3.2.9. Cell Lysate Preparation and Immunoblotting

Cells were homogenized in 25 mM Hepes buffer, pH 7.8, 300 mM NaCl, 1.5 mM MgCl2, 1% Triton X-100, 0.1 mM DTT, 0.2 mM PMSF, containing 1:100 protease inhibitor mixture without EDTA (Sigma). Cellular debris was removed by centrifugation at 10,000 %g for 15 min at 4 °C. Thirty micrograms of total protein lysate was incubated with 10 units of shrimp alkaline phosphatase (Fermentas) for 30 min at 37 °C. At the end of the incubation, 5% SDS sample buffer was added and the sample was loaded on SDS/PAGE.

3.2.10. Statistical Analysis

A two-way ANOVA followed by Bonferroni posttest was used to compare treatment groups in the accelerated rotarod, narrow, beam, and horizontal ladder tests, as well as in the analysis of DARPP-32 expression. The Wilcoxon test (nonparametric) was used to analyze data from the rotarod task at fixed speed. Two-tailed t test was used to compare the mean fluorescence intensity of GM1-treated versus GM1-untreated samples in immunocytochemistry experiments and in all other experiments.

3.3. RESULTS

3.3.1. Chronic Infusion of GM1 Restores Normal Motor Behavior in YAC128 Mice

To assess the therapeutic potential of GM1 in HD, and to avoid potential confounding effects from peripheral drug administration and limited blood–brain barrier permeability, we developed a protocol for chronic intraventricular infusion of the ganglioside in a well-characterized transgenic mouse model of HD, the YAC128 mouse. YAC128 mice express the full-length mutant huntingtin protein and recapitulate the motor deficit and other salient features of the human pathology (37). YAC128 and wild-type littermates were infused with GM1 or vehicle (artificial cerebrospinal fluid, CSF) for 28 d. Motor behaviour was analyzed before and at various time points during the infusion period. Chronic infusion of GM1 restored normal GM1 levels in the striatum and the cortex of YAC128 mice (Figure 3.1).

At the time when the treatment with ganglioside GM1 was initiated, 5-mo-old YAC128 mice already showed severe motor impairment compared with wild-type (WT) littermates (Figure 3.2A, C, and D, time point −4 in all graphs), as assessed using a battery of motor behavior tests. These included the rotarod, a gold standard in the qualitative analysis of motor behavior in HD mice, as well as the horizontal ladder walking test and the narrow beam, two highly discriminatory motor tests for the assessment of cortical and subcortical dysfunction (38, 39).

Remarkably, after 2 wk of GM1 intraventricular infusion, normal motor function was recovered in YAC128 mice compared with WT littermates, in all of the tests performed (Figure 3.2).

At fixed rotarod speed (20 rpm), YAC128 mice were able to remain on the rotarod for less than 30 s. As expected, intraventricular infusion of artificial CSF vehicle did not improve their performance. On the contrary, YAC128 mice that received GM1 improved dramatically and by the end of the

treatment could finish the 60-s test like most of the WT mice (Figure 3.2A). As this test was only moderately challenging for WT mice and we wanted to assess the true extent of recovery in YAC128 mice, we repeated the test with an accelerating rotarod, in conditions that were very challenging even for WT mice (from 4 to 40 rpm in 1 min). Even in these conditions, GM1-treated YAC128 mice performed similarly to WT littermates (differences were not statistically significant) (Figure 3.2B).

Complete rescue of normal motor functions was also observed when YAC128 mice were tested in the horizontal ladder walking task (Figure 3.2C) and in the narrow beam test (Figure 3.2D), which require balance and fine motor skills (38, 39). The beneficial effects of GM1 extended up to 14 d after discontinuation of the treatment (Figure 3.3).

No effects on motor behavior were observed in WT mice infused with GM1 or in YAC128 mice infused with the artificial CSF vehicle (Figure 3.2). Importantly, no evident signs of treatment-related toxicity or illness were detected at any time during the experimental protocol.

3.3.2. GM1 Increases DARPP-32 Expression and Activation in the Striatum of YAC128 Mice

DARPP-32 is highly enriched in medium-sized spiny neurons and its down-regulation is an early marker of neuronal dysfunction in HD (40). Normalization of motor behavior in GM1-treated YAC128 mice correlated with increased striatal expression of DARPP-32 (Figure 3.4). Treatment with GM1 also restored normal levels of DARPP-32 phoshorylation at threonine 34 in the striatum of YAC128 mice, suggesting overall normalization of cell signaling and/or dopaminergic pathways in medium spiny neurons (41, 42).

3.3.3. GM1 Triggers Phosphorylation of Huntingtin at Serine 13 and Serine 16

The dramatic effects exerted by GM1 in YAC128 mice suggest that the

ganglioside might decrease overall mutant huntingtin toxicity. As phosphomimetic mutations of serine 13 and serine 16 result in abrogation of mutant huntingtin toxicity in a BACHD model (17), we tested whether GM1 could increase phosphorylation of huntingtin at these two critical amino acid residues. Using a phospho-specific antibody (pN17) (16) that recognizes the amino-terminal N17 domain of huntingtin (the first 17 amino acids) only when serine 13 and serine 16 are phosphorylated, we detected a significant increase of huntingtin phosphorylation at serines 13 and 16 in primary cultures of neurons isolated from YAC128 or WT littermates, by immunocytochemistry (Figure 3.5A) and immunoblotting (Figure 3.6A), after incubation with GM1 for 5 h.

Similar results were obtained using immortalized striatal homozygous knock-in cells expressing mutant huntingtin ($STHdh^{111/111}$ cells; Figure 3.5B).

Thus, GM1 can induce phosphorylation of huntingtin at those critical residues both in normal and HD cells. Treatment with the ganglioside triggered huntingtin phosphorylation also in fibroblasts derived from HD patients (Figure 3.5C and Figure 3.6B), demonstrating that the underlying mechanism is shared between animal and human models and that a GM1- based therapy is likely to have beneficial effects in HD patients.

We confirmed that GM1 induces phosphorylation at serines 13 and 16 by incubation of striatal knock-in cells ($STHdh^{111/111)}$ with GM1, followed by immunoprecipitation of mutant huntingtin with a polyclonal anti-huntingtin antibody (16) and immunoblotting with three phospho-specific antibodies: pN17 (16) and anti-pSer13 and anti-pSer16 antibodies (10), which recognize phosphoserine 13 and phosphoserine 16, respectively (Figure 3.5D). Increased huntingtin phosphorylation at serine 13 and serine 16 after treatment with GM1 was also detected after direct immunoprecipitation of phospho huntingtin using pN17 antibodies (Figure 3.5E). More phosphohuntingtin was immunoprecipitated with pN17 after treatment with GM1 and the results were confirmed by immunoblotting with anti-pSer13 and anti-pSer16 antibodies.

Interestingly, on SDS/PAGE analysis, phosphohuntingtin consistently migrated at a much higher apparent molecular weight (hmw-Htt) (Figs. 3.5D and 3.5E) than the monomeric full-length huntingtin (FL-Htt), regardless of the length of the polyglutamine stretch (Figure 3.5F and Figure 3.6) and consistent with the formation of a high molecular-weight protein complex or huntingtin dimers. All anti-huntingtin and anti-phosphohuntingtin antibodies used in this study recognized the complex, although mAb2166 with low affinity. A positive signal with mAb2166 was seen in most cases only after overexposure of the immunoblot (Figure 3.5E). This is not surprising as binding of mAb2166 antibodies has been shown to be affected by huntingtin conformational changes induced by expansion of the polyQ stretch (43) and/or huntingtin posttranslational modifications (10). Phosphorylation of huntingtin was required for the formation and/or stabilization of the high molecular-weight huntingtin complex, both in wild-type and HD cells, because dephosphorylation of the cell lysate with shrimp alkaline phosphatase (SAP) resulted in a decrease of the high molecular-weight form of huntingtin and the increase of monomeric full-length huntingtin levels (Figure 3.5F). Confirming our in vitro studies, GM1 treatment resulted in a significant increase in huntingtin phosphorylation at serine 13 and 16 in vivo in the cortex and striatum of both YAC128 and WT mice that were chronically infused with GM1 (Figure 3.7).

3.4. DISCUSSION

The complexity and variety of cellular pathways that are affected in HD has long hampered the development of effective therapies for this disease. In recent years, the discovery that posttranslational modifications can dramatically affect mutant huntingtin toxicity has opened the door to novel potential therapeutic strategies that target cell signaling pathways and factors responsible for critical huntingtin protein modifications. GM1 is a lipid with important modulatory roles in the nervous system (18). In HD, decreased levels of this and other gangliosides, as we recently reported (19), are likely to affect cell signaling and neuronal function. Our previous studies showed that in a knock-in cell model expressing full-length mutant huntingtin, decreased levels of ganglioside GM1 contributed to heightened cell susceptibility to apoptosis. Restoring normal GM1 levels reverted the phenotype of HD cells to normal, suggesting that GM1 could have a therapeutic action in HD models. The in vivo studies herein described strongly support this conclusion. To date, GM1 is the only treatment that leads to a complete rescue of the motor phenotype in an HD mouse model, even after disease onset. At the time when the treatment was initiated, YAC128 mice already displayed profound motor deficits (Figure 3.2), yet GM1 infusion was able to restore normal motor functions in 14 d of treatment. Interestingly, GM1-treated YAC128 mice performed significantly better than CSF-treated mice for over 14 d after discontinuation of the treatment (Figure 3.2). These results suggest that GM1 is able to decrease mutant huntingtin toxicity and to correct abnormal homeostatic mechanisms that develop over time and that are responsible for the overall malfunction, and eventually death of HD neurons. These conclusions are also supported by our data showing that GM1 restores normal levels of DARPP- 32 expression and phosphorylation in the striatum of YAC128 mice (Figure 3.4.). Decreased DARPP-32 expression is an early sign of neuronal dysfunction in the R6/2 mouse model of HD (40), and has also been reported in YAC128 mice (44). DARPP-32 plays a crucial role at the

crossroad of dopaminergic and other signaling pathways, which converge to determine overall expression level and phosphorylation state (resulting in specific protein functions) of DARPP-32 in medium spiny neurons. In turn, DARPP-32 integrates neuronal responses to a variety of neurotransmitters and stimuli and modulates striatum output pathways (41, 42, 45). Restoring normal GM1 concentration in the brain of YAC128 mice likely resulted in a plethora of beneficial effects, leading to the therapeutic endpoints described in this study. The extent of such effects also suggests that GM1 targets early steps in the cascade of pathogenic events triggered by mutant huntingtin in HD brains. Indeed, we found that GM1 affects mutant huntingtin itself, by increasing phosphorylation at huntingtin serine 13 and serine 16 (Figs. 3.5., 3.6. and 3.7.). In vitro studies have shown that concomitant phosphorylation of these two amino acid residues decreases the toxicity of mutant huntingtin (10, 16). In vivo, phosphomimetic mutations at the same amino acids protect BACHD transgenic models from the development of HD-like pathology. Thus, mutant huntingtin phosphorylation at these critical sites might explain, at least in part, the therapeutic action of GM1 in HD mice. It has been proposed that huntingtin phosphorylation at serine 13 and serine 16 might decrease mutant huntingtin toxicity by changing protein conformation (16, 17), huntingtin function (16), and/or rate of huntingtin degradation (10). In a recent study, N-terminal fragments of mutant huntingtin in which serine 16 was changed to aspartic acid (mimicking phosphorylation at serine 16), were shown to preferentially accumulate and form aggregates in the cell nucleus. Although the consequences of huntingtin serine 16 phosphorylation on cell viability were not assessed in that study, it was proposed that phosphorylation at this amino acid residue might be important for toxicity mediated by mutant huntingtin fragments (46). Thus, the consequences of huntingtin phosphorylation at serine 16 on cell functions and viability might depend on whether only serine 16 (46) or both serine 13 and 16 (16, 17, 47, and this study) are phosphorylated, on protein context (full-length huntingtin versus N-terminal fragments) and, potentially, on the co-occurrence of other

concomitant posttranslational modifications of mutant huntingtin (2, 10, 17, 48). Elucidating the signaling pathways involved in regulating huntingtin posttranslational modifications and their cross-talk will be of utmost importance. In our studies we observed that huntingtin phosphorylated at serine 13 and serine 16 consistently migrated at higher molecular weight than predicted, consistent with the formation of an SDS–insoluble protein complex or dimer. The ability of huntingtin to form homodimers has been predicted by computational analysis and demonstrated in a yeast two-hybrid system using huntingtin fragments (49), and in preparations of full-length huntingtin purified from an insect cell expression system (50). Currently, the relevance of the formation of a high molecular-weight huntingtin complex or protein dimerization to huntingtin function is unknown. We found that the ability to detect the high molecular-weight form of huntingtin by immunoblotting depends on protein transfer conditions (Materials and Methods), perhaps explaining why only in a few other studies this form of huntingtin was detected (but not highlighted) (10, 51, 52). In conclusion, our data support the use of GM1 in clinical setting for the treatment of HD. In this regard, previous clinical trials in which the ganglioside was used for the treatment of other conditions (35, 53–55) demonstrated that GM1 is safe to use in patients, even when administered by intraventricular infusion (56), and potential adverse effects are rare (35).

3.5. **FIGURES**

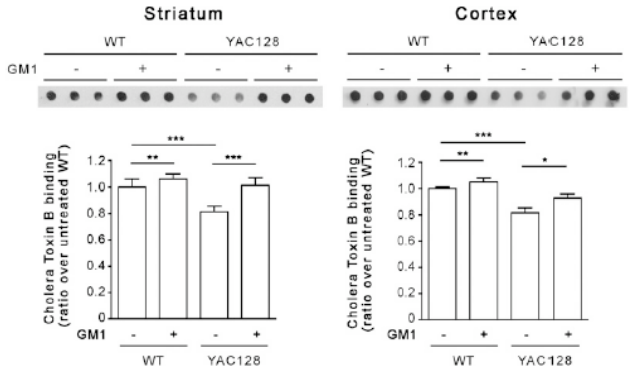

Figure 3.1. Chronic GM1 infusion restores normal GM1 levels in the striatum and cortex of YAC128 mice. Representative dot blots of equal amounts of striatum and brain cortex lysates prepared from 6-mo-old YAC128 mice and wild-type littermates treated with GM1 or CSF for 28 d. GM1 levels were detected by cholera toxin B binding. Each dot represents one animal. Graphs show the mean densitometric values **±**SD (n = 6 mice per experimental group). *P **<** 0.05; **P **<** 0.001; ***P **<** 0.0001.

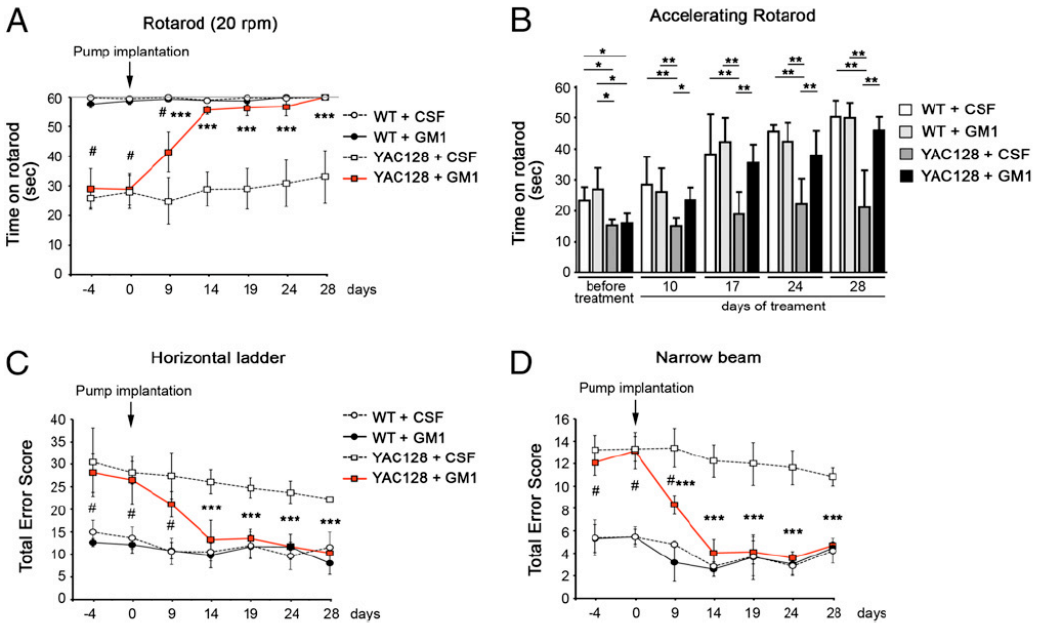

Figure 3.2. GM1 restores normal motor behavior in YAC128 mice. Behavioral tests were conducted at the indicated time, on 5-mo-old YAC128 and WT mice, before and during GM1 chronic brain infusion. Each data point represents the average performance ±SD of six mice. (**A**) Rotarod test at fixed speed (20 rpm for 60 s). YAC128 mice treated with GM1 showed progressive improvement and, by the end of the treatment, were able to finish the test like most WT mice. The horizontal gray line in the graph marks the test endpoint. (**B**) Accelerating rotarod (4–40 rpm in 1 min). In this challenging test, YAC128 mice treated with GM1 performed as well as WT mice (differences between WT and GM1-treated YAC128 mice were not statistically significant). (**C**) Horizontal ladder test. The ability of mice to cross a horizontal ladder with irregular rung pattern was analyzed. A score was assigned to each type of footfall and other mistakes made by the mice according to ref. 38. (**D**) Narrow beam test. Motor performance was scored as the mice walked along a narrow beam (100 cm long, 0.75 cm wide). **#P <** 0.01 (YAC128 vs. WT); ***P <** 0.05; ****P <** 0.01; *****P <** 0.001 (GM1-treated vs. CSF-treated YAC128).

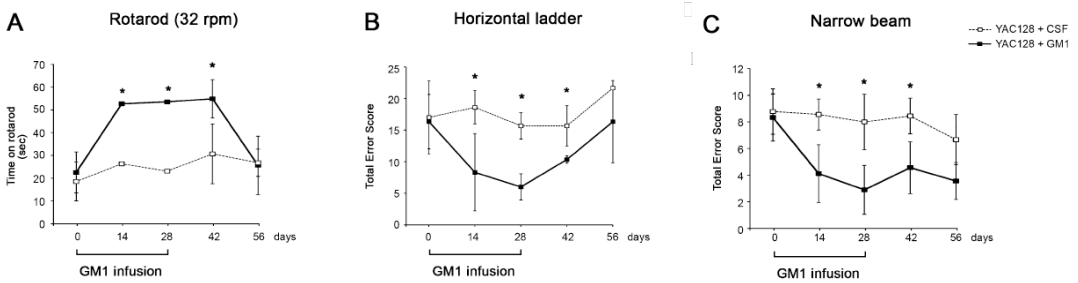

Figure 3.3. Sustained beneficial effect of GM1 after treatment discontinuation. YAC128 mice that were infused with GM1 for 28 d performed significantly better than YAC128 mice infused with CSF, in all motor tests, up to 14 d after discontinuation of the treatment. Each point in the graphs represents the average performance ±SD of three mice. *P < 0.05.

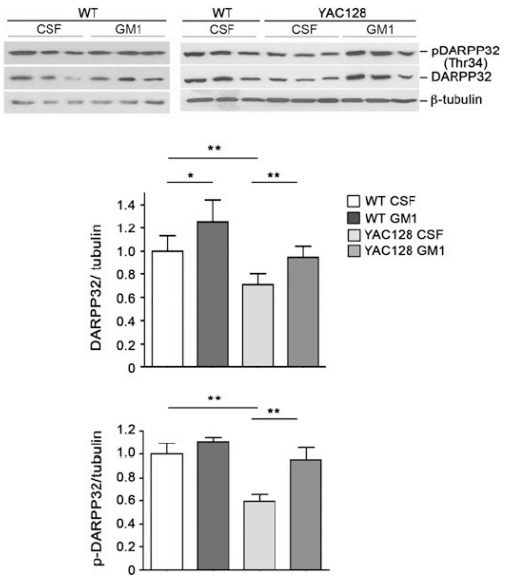

Figure 3.4. GM1 restores striatal expression of DARPP-32 in YAC128 mice. Representative immunoblot and Li-Cor Odissey densitometric analysis of DARPP-32 expression and activation (p-DARPP-32) in WT and YAC128 mice. GM1 infusion for 28 d restores normal levels of DARPP-32 and active p- DARPP-32 in YAC128 mice. Each lane of the immunoblot represents one individual mouse. Graphs show the densitometric analysis performed on three (WT GM1) or six (all other experimental groups) mice per group. Bars represent the mean values ±SD *P < 0.05; **P < 0.01.

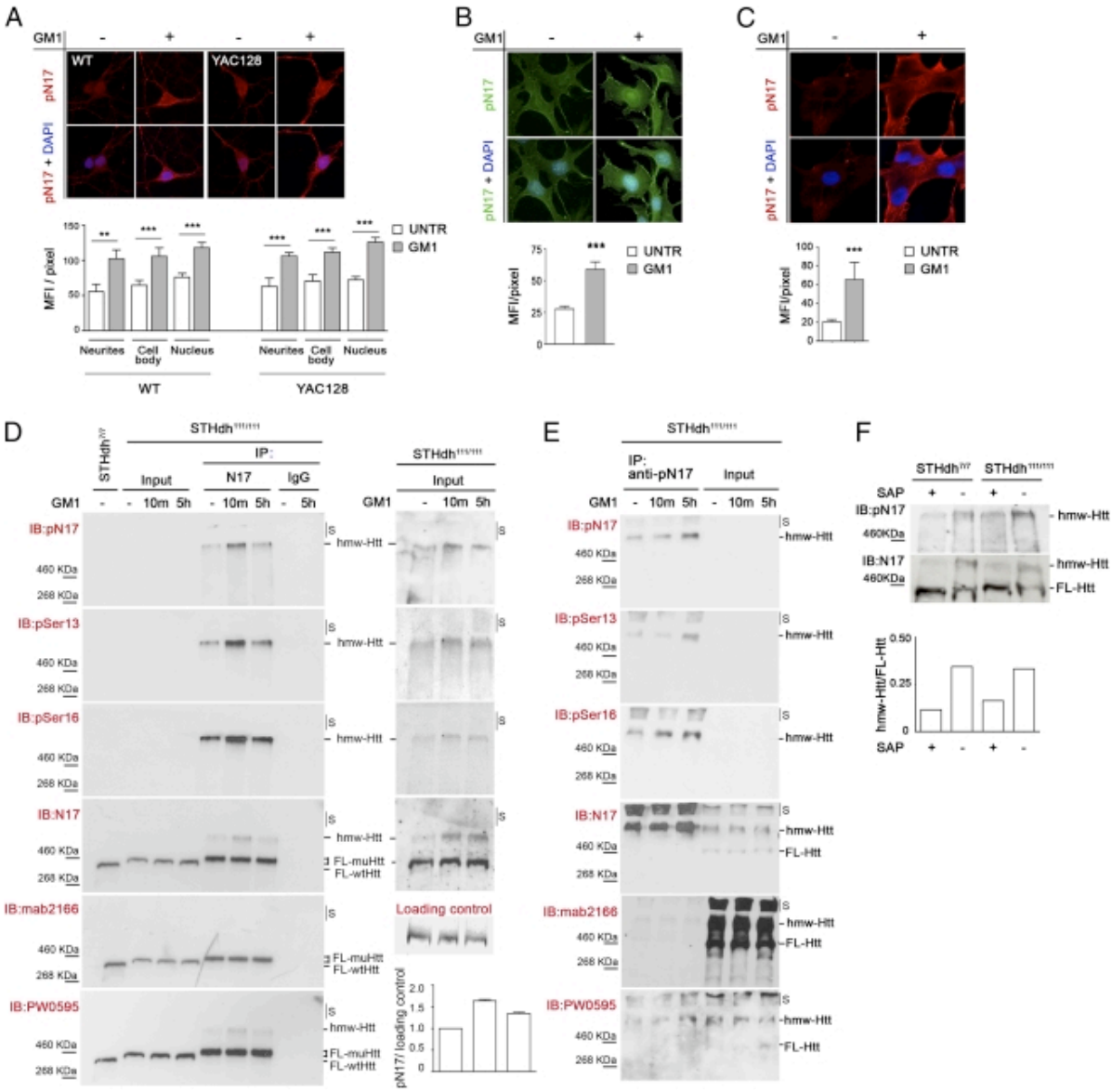

Figure 3.5. GM1 administration elicits huntingtin phosphorylation at serine 13 and serine 16 (*A*) Representative confocal microscopy images and relative quantitative analysis of primary striatal neurons isolated from wild-type (WT) and YAC128 mice and incubated for 5 h with 50 M GM1 (+) or vehicle (&). Neurons were immunostained with anti–phospho-N17 (pN17) antibody, which recognizes the amino-terminal N17 peptide of huntingtin phosphorylated at amino acid residues serine 13 and serine 16, and with DAPI to visualize nuclei. (*B*) Representative epifluorescence microscope images and quantitative analysis of immortalized knock-in striatal progenitor cells expressing mutant huntingtin (ST*Hdh*$^{111/111}$) and treated as in *A*. (*C*) Confocal microscopy images and quantitative analysis of primary fibroblasts from HD patients treated as in *A*. Graphs in *A*–*C* show pN17 immunostaining

mean fluorescence intensity (MFI) per pixel ±SD, calculated over a minimum of 100 cells per experimental group. $^{**}P < 0.01$; $^{***}P < 0.001$. (*D* and *E*) Analysis of mutant huntingtin phosphorylation state by immunoprecipitation and immunoblotting. Striatal knock-in cells (ST*Hdh*$^{111/111}$) were incubated with 50 M GM1 for the indicated time (10m, 10 min). Mutant huntingtin was immunoprecipitated from equal amounts of total cell lysates using a rabbit polyclonal anti-huntingtin antibody (N17) (in *D*), phospho-specific pN17 antibodies (in *E*), or nonspecific rabbit IgG antibodies as negative control (*D*). Total lysate from cells expressing wild-type huntingtin (ST*Hdh*$^{7/7}$) was loaded in the same gel as reference. All immunoprecipitated material (IP) was immunoblotted with the indicated phospho-specific and anti-huntingtin antibodies. Phosphohuntingtin could not be detected in the total lysates (input lanes, 30 g of proteins loaded) due to the proximity of the highly immune-reactive immunoprecipitated material in adjacent lanes. The results of reprobing the input lanes only, after cutting the membrane, are shown in *D*, *Right*. An increase in the phosphorylation of huntingtin at serine 13 and serine 16 after treatment with GM1 is evident in both immunoprecipitated material and input total cell lysates. The graph in *D* shows the densitometric analysis of huntingtin phosphorylation in the input lysates of two independent experiments. A Ponceau red-stained band in the membrane was used as loading control. S, stacking portion of the gel. (*F*) Wild-type and mutant huntingtin in total cell lysate from striatal knock-in cells (ST*Hdh*$^{7/7}$ and ST*Hdh*$^{111/111}$) was dephosphorylated using shrimp alkaline phosphatase (SAP). Dephosphorylation resulted in a dramatic change in huntingtin electrophoretic mobility, with increased amount of protein migrating at the lower apparent molecular weight (FL-Htt) and a decreased amount of high molecular-weight species (hmw-Htt). The graph shows the ratio between hmw-Htt and FL-Htt before and after dephosphorylation with SAP.

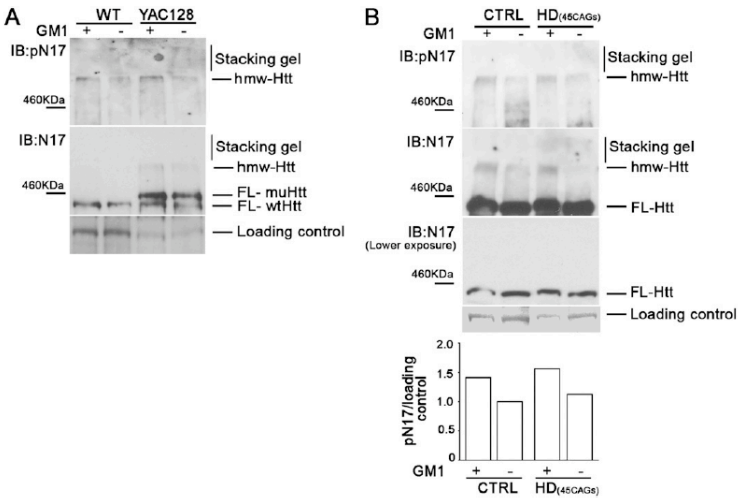

Figure 3.6. GM1 administration promotes huntingtin phosphorylation at serine 13 and serine 16 in primary cultures of neurons and human fibroblasts. (**A**) Primary striatal neurons isolated from wild-type (WT) and YAC128 mice were incubated for 5 h with 50 M GM1 (+) or vehicle (−). Total lysates were immunoblotted with phospho-specific pN17 antibodies and with polyclonal anti-Htt (N17) antibodies. Loading control is a nonspecific protein band detected by antitalin antibodies. (**B**) Primary fibroblasts isolated from a healthy control subject and from a HD patient (expressing 45 CAG repeats in the mutant HD gene) were treated as in **A**. Total cell lysates were immunoblotted with pN17 and anti-Htt (N17) antibodies. The graph shows the densitometric analysis of phosphohuntingtin, normalized over the loading control (Ponceau red-stained protein band). Hmw-Htt, high molecular-weight huntingtin; FL-Htt, full-length huntingtin; FL-wtHtt, full-length wild-type huntingtin; FL-muHtt, full-length mutant huntingtin.

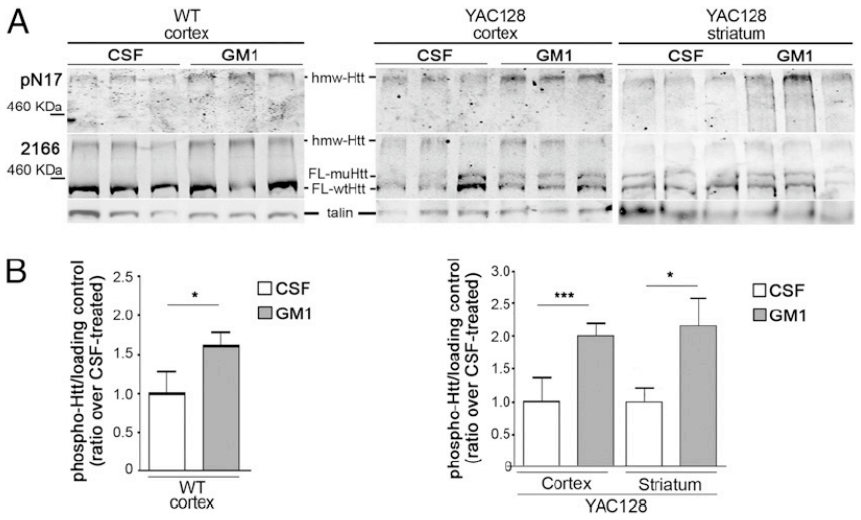

Figure 3.7. GM1 infusion induces huntingtin phosphorylation in vivo. Total protein lysates were prepared from the cortex and the striatum of YAC128 mice and WT littermates chronically infused with artificial cerebrospinal fluid (CSF) or GM1 in CSF for 28 d (six mice per group). (**A**) Representative immunoblots showing increased phosphorylation of huntingtin at serine 13 and serine 16 in GM1-infused brains, as detected using pN17 antibody. Each lane corresponds to the lysate from one mouse. (**B**) Li-Cor Odyssey infrared densitometric analysis of phosphohuntingtin normalized over talin (loading control). Bars represent the mean ± SD of six mice per experimental group. *p< 0.05; ***p < 0.001.

3.6. **REFERENCES**

1. Zuccato C, Valenza M, Cattaneo E (2010) Molecular mechanisms and potential therapeutical targets in Huntington's disease. Physiol Rev 90:905–981.
2. Steffan JS, et al. (2004) SUMO modification of Huntingtin and Huntington's disease pathology. Science 304:100–104.
3. Graham RK, et al. (2006) Cleavage at the caspase-6 site is required for neuronal dysfunction and degeneration due to mutant huntingtin. Cell 125:1179–1191.
4. Jeong H, et al. (2009) Acetylation targets mutant huntingtin to autophagosomes for degradation. Cell 137:60–72.
5. Schilling B, et al. (2006) Huntingtin phosphorylation sites mapped by mass spectrometry. Modulation of cleavage and toxicity. J Biol Chem 281:23686–23697.
6. Luo S, Vacher C, Davies JE, Rubinsztein DC (2005) Cdk5 phosphorylation of huntingtin reduces its cleavage by caspases: Implications for mutant huntingtin toxicity. J Cell Biol 169:647–656.
7. Warby SC, et al. (2009) Phosphorylation of huntingtin reduces the accumulation of its nuclear fragments. Mol Cell Neurosci 40:121–127.
8. Anne SL, Saudou F, Humbert S (2007) Phosphorylation of huntingtin by cyclin-dependent kinase 5 is induced by DNA damage and regulates wild-type and mutant huntingtin toxicity in neurons. J Neurosci 27:7318–7328.
9. Rangone H, et al. (2004) The serum- and glucocorticoid-induced kinase SGK inhibits mutant huntingtin-induced toxicity by phosphorylating serine 421 of huntingtin. Eur J Neurosci 19:273–279.
10. Thompson LM, et al. (2009) IKK phosphorylates Huntingtin and targets it for degradation by the proteasome and lysosome. J Cell Biol 187:1083–1099.
11. Zala D, et al. (2008) Phosphorylation of mutant huntingtin at S421 restores anterograde and retrograde transport in neurons. Hum Mol Genet 17:3837–3846.
12. Atwal RS, et al. (2007) Huntingtin has a membrane association signal that can modulate huntingtin aggregation, nuclear entry and toxicity. Hum Mol Genet 16: 2600–2615.
13. Rockabrand E, et al. (2007) The first 17 amino acids of Huntingtin modulate its subcellular localization, aggregation and effects on calcium homeostasis. Hum Mol Genet 16:61–77.
14. Lakhani VV, Ding F, Dokholyan NV (2010) Polyglutamine induced misfolding of huntingtin exon1 is modulated by the flanking sequences. PLOS Comput Biol 6: e1000772.
15. Thakur AK, et al. (2009) Polyglutamine disruption of the huntingtin exon 1 N terminustriggers a complex aggregation mechanism. Nat Struct Mol Biol 16:380–389.
16. Atwal RS, et al. (2011) Kinase inhibitors modulate huntingtin cell localization and

toxicity. Nat Chem Biol 7:453–460.
17. Gu X, et al. (2009) Serines 13 and 16 are critical determinants of full-length human mutant huntingtin induced disease pathogenesis in HD mice. Neuron 64:828–840.
18. Posse de Chaves E, Sipione S (2009) Sphingolipids and gangliosides of the nervous system in membrane function and dysfunction. FEBS Lett 584:1748–1759.
19. Maglione V, et al. (2010) Impaired ganglioside metabolism in Huntington's disease and neuroprotective role of GM1. J Neurosci 30:4072–4080.
20. Desplats PA, et al. (2007) Glycolipid and ganglioside metabolism imbalances in Huntington's disease. Neurobiol Dis 27:265–277.
21. Denny CA, Desplats PA, Thomas EA, Seyfried TN (2010) Cerebellar lipid differences between R6/1 transgenic mice and humans with Huntington's disease. J Neurochem 115:748–758.
22. Simons K, Toomre D (2000) Lipid rafts and signal transduction. Nat Rev Mol Cell Biol 1: 31–39.
23. Sonnino S, Mauri L, Chigorno V, Prinetti A (2007) Gangliosides as components of lipid membrane domains. Glycobiology 17:1R–13R.
24. Hakomori Si SI (2002) The glycosynapse. Proc Natl Acad Sci USA 99:225–232.
25. Yoon SJ, Nakayama K, Hikita T, Handa K, Hakomori SI (2006) Epidermal growth factor receptor tyrosine kinase is modulated by GM3 interaction with N-linked GlcNAc termini of the receptor. Proc Natl Acad Sci USA 103:18987–18991.
26. Oblinger JL, Boardman CL, Yates AJ, Burry RW (2003) Domain-dependent modulation of PDGFRbeta by ganglioside GM1. J Mol Neurosci 20:103–114.
27. Toledo MS, Suzuki E, Handa K, Hakomori S (2005) Effect of ganglioside and tetraspanins in microdomains on interaction of integrins with fibroblast growth factor receptor. J Biol Chem 280:16227–16234.
28. Mocchetti I (2005) Exogenous gangliosides, neuronal plasticity and repair, and the neurotrophins. Cell Mol Life Sci 62:2283–2294.
29. Fantini J, Barrantes FJ (2009) Sphingolipid/cholesterol regulation of neurotransmitter receptor conformation and function. Biochim Biophys Acta 1788:2345–2361.30. Ledeen RW, Wu G (2008) Nuclear sphingolipids: Metabolism and signaling. J Lipid Res 49:1176–1186.
30. Ledeen RW, Wu G (2008) Nuclear sphingolipids: Metabolism and signaling. J Lipid Res 49:1176–1186.
31. Wu G, Xie X, Lu ZH, Ledeen RW (2009) Sodium-calcium exchanger complexed with GM1 ganglioside in nuclear membrane transfers calcium from nucleoplasm to endoplasmic reticulum. Proc Natl Acad Sci USA 106:10829–10834.
32. Mehta NR, Nguyen T, Bullen JW, Jr., Griffin JW, Schnaar RL (2010) Myelin-

associated glycoprotein (MAG) protects neurons from acute toxicity using a ganglioside-dependent mechanism. ACS Chem Neurosci 1:215–222.

33. Schnaar RL (2010) Brain gangliosides in axon-myelin stability and axon regeneration. FEBS Lett 584:1741–1747.
34. Susuki K, et al. (2007) Gangliosides contribute to stability of paranodal junctions and ion channel clusters in myelinated nerve fibers. Glia 55:746–757.
35. Alter M (1998) GM1 ganglioside for acute ischemic stroke. Trial design issues. Ann N Y Acad Sci 845:391–401.
36. Squitieri F, Frati L, Ciarmiello A, Lastoria S, Quarrell O (2006) Juvenile Huntington's disease: Does a dosage-effect pathogenic mechanism differ from the classical adult disease? Mech Ageing Dev 127:208–212.
37. Slow EJ, et al. (2003) Selective striatal neuronal loss in a YAC128 mouse model of Huntington disease. Hum Mol Genet 12:1555–1567.
38. Metz GA, Whishaw IQ (2002) Cortical and subcortical lesions impair skilled walking in the ladder rung walking test: A new task to evaluate fore- and hindlimb stepping, placing, and co-ordination. J Neurosci Methods 115:169–179.
39. Metz GA, Merkler D, Dietz V, Schwab ME, Fouad K (2000) Efficient testing of motor function in spinal cord injured rats. Brain Res 883:165–177.
40. Bibb JA, et al. (2000) Severe deficiencies in dopamine signaling in presymptomatic Huntington's disease mice. Proc Natl Acad Sci USA 97:6809–6814.
41. Reis HJ, et al. (2007) Is DARPP-32 a potential therapeutic target? Expert Opin Ther Targets 11:1649–1661.
42. Svenningsson P, et al. (2004) DARPP-32: An integrator of neurotransmission. Annu Rev Pharmacol Toxicol 44:269–296.
43. Wheeler VC, et al. (2000) Long glutamine tracts cause nuclear localization of a novel form of huntingtin in medium spiny striatal neurons in HdhQ92 and HdhQ111 knockin mice. Hum Mol Genet 9:503–513.
44. Metzler M, et al. (2010) Phosphorylation of huntingtin at Ser421 in YAC128 neurons is associated with protection of YAC128 neurons from NMDA-mediated excitotoxicity and is modulated by PP1 and PP2A. J Neurosci 30(43):14318–14329.
45. Nishi A, Kuroiwa M, Shuto T (2011) Mechanisms for the modulation of dopamine d(1) receptor signaling in striatal neurons. Front Neuroanat 5:43.
46. Havel LS, et al. (2011) Preferential accumulation of N-terminal mutant huntingtin in the nuclei of striatal neurons is regulated by phosphorylation. Hum Mol Genet 20: 1424–1437.
47. Bernardo A, et al. (2009) Elimination of GD3 synthase improves memory and reduces amyloid-beta plaque load in transgenic mice. Neurobiol Aging 30:1777–1791.

48. Aiken CT, et al. (2009) Phosphorylation of threonine 3: Implications for Huntingtin aggregation and neurotoxicity. J Biol Chem 284:29427–29436.
49. Palidwor GA, et al. (2009) Detection of alpha-rod protein repeats using a neural network and application to huntingtin. PLOS Comput Biol 5:e1000304.
50. Li W, Serpell LC, Carter WJ, Rubinsztein DC, Huntington JA (2006) Expression and characterization of full-length human huntingtin, an elongated HEAT repeat protein. J Biol Chem 281:15916–15922.
51. Dyer RB, McMurray CT (2001) Mutant protein in Huntington disease is resistant to proteolysis in affected brain. Nat Genet 29:270–278.
52. Wood JD, MacMillan JC, Harper PS, Lowenstein PR, Jones AL (1996) Partial characterization of murine huntingtin and apparent variations in the subcellular localization of huntingtin in human, mouse and rat brain. Hum Mol Genet 5:481–487.
53. Schneider JS (1998) GM1 ganglioside in the treatment of Parkinson's disease. Ann N Y Acad Sci 845:363–373.
54. Chinnock P, Roberts I (2005) Gangliosides for acute spinal cord injury. Cochrane Database Syst Rev (2):CD004444.
55. Schneider JS, Sendek S, Daskalakis C, Cambi F (2010) GM1 ganglioside in Parkinson's disease: Results of a five year open study. J Neurol Sci 292:45–51.
56. Svennerholm L, et al. (2002) Alzheimer disease: effect of continuous intracerebroventricular treatment with GM1 ganglioside and a systematic activation programme. Dement Geriatr Cogn Disord 14:128–136.
57. Pardridge W (1991) Transnasal and intraventricular delivery. Peptide Drug Delivery to the Brain (Raven Press, San Diego), p 112.

4. CONCLUDING REMARKS

This thesis has been inspired by the lack of clear understanding of the crucial molecular mechanisms underlying the pathogenesis of HD and the need to identify potential therapeutic strategies. Numerous are the alterations of essential biological processes that have been reported to contribute to the pathophysiology of HD, and many are the agents so far identified that provide some therapeutic benefits, at least in animal models of the disease. However, therapeutic options remain severely limited, with only symptomatic therapies available. A better understanding of key mechanisms causative of HD may help to identify new molecular targets for the development of more effective therapeutic solutions.

The first part of this thesis aimed at clarifying the molecular mechanism causing dysfunction of the cholesterol biosynthetic pathway in HD. The results obtained indicate that mHtt leads to aberrant cholesterol biosynthesis by interfering with the normal activity of SREBP2, the transcription factor involved in the regulation of intracellular cholesterol homeostasis. Mutant Htt interacts with SREBP2 and retains it in the cytoplasm, inhibiting its nuclear transport and ultimately expression of target genes. Based on this knowledge,

interventions that block the interaction of mHtt with SREBP2 might have therapeutic benefits in HD.

In the second part of the thesis, I evaluated the administration of ganglioside GM1, as a valid and innovative approach for the treatment of HD. The results obtained with GM1 are encouraging with regard to the beneficial effects of this molecule in HD models. Not only GM1 restored normal motor behavior in YAC128 mice, but also triggered phosphorylation of mHtt at serine 13 and serine 16, a post-translational modification known to decrease mHtt toxicity. This suggest that GM1 might be a disease modifying treatment able not only to restore normal GM1 levels in HD brains, but also to attenuate other molecular dysfunctions associated with expression of mHtt, including cholesterol metabolism dysfunction, and to slow down disease progression.

My studies have shown that restoring GM1 levels in HD brains is feasibile and is not associated to obvious signs of toxicity. However, delivery of gangliosides into the brain is challenging, since only small amounts of GM1 administered peripherally are able to cross the blood-brain barrier. In my studies I took advantage of stereotaxic procedures and intracerebroventricular infusion kits to deliver GM1 into the brain ventricules. This represents a quite invasive and challenging approach that, although feasible, would limit the use of GM1 for the treatment of HD patients. Alternative routes of administration would have to be evaluated, in parallel with the development of second-generation molecules with improved pharmacokinetic profiles.